British Journal of Pharmacology

British Journal of Pharmacology (2016) **173** 3041–3079 3041

REVIEW ARTICLE

The therapeutic and diagnostic potential of the prostate specific membrane antigen/glutamate carboxypeptidase II (PSMA/GCPII) in cancer and neurological disease

Correspondence Professor Caitriona O'Driscoll, School of Pharmacy, University College Cork T12 YT20, Ireland. E-mail: caitriona.odriscoll@ucc.ie

Received 14 May 2016; **Revised** 8 July 2016; **Accepted** 25 July 2016

James C Evans[1], Meenakshi Malhotra[1], John F Cryan[2] and Caitriona M O'Driscoll[1]

[1]*Pharmacodelivery Group, School of Pharmacy, University College Cork, Cork, Ireland, and* [2]*Department of Anatomy and Neuroscience, University College Cork, Cork, Ireland*

Prostate specific membrane antigen (PSMA) otherwise known as glutamate carboxypeptidase II (GCPII) is a membrane bound protein that is highly expressed in prostate cancer and in the neovasculature of a wide variety of tumours including glioblastomas, breast and bladder cancers. This protein is also involved in a variety of neurological diseases including schizophrenia and ALS. In recent years, there has been a surge in the development of both diagnostics and therapeutics that take advantage of the expression and activity of PSMA/GCPII. These include gene therapy, immunotherapy, chemotherapy and radiotherapy. In this review, we discuss the biological roles that PSMA/GCPII plays, both in normal and diseased tissues, and the current therapies exploiting its activity that are at the preclinical stage. We conclude by giving an expert opinion on the future direction of PSMA/GCPII based therapies and diagnostics and hurdles that need to be overcome to make them effective and viable.

Abbreviations

2-MPPA, 2-(3-mercaptopropyl)pentanedioic acid; 2-PMPA, 2-(phosphonomethyl)pentanedioic acid; aa, amino acids; ADC, antibody-drug conjugate; AR, androgen receptor; BBB, blood–brain barrier; CAR, chimeric antigen receptor; CTL, cytotoxic T-lymphocyte; DCs, Dendritic cells; DHT, dihydrotestosterone; dsRNA, double stranded RNA; FBP, folate-binding proteins; FLNa, filamin A; FOLH1, folate hydrolase; hNIS, human sodium iodide symporter; huPSMA, expressing human PSMA; KD, knockdown; mGLU, metabotropic glutamate receptors; NAA, N-acetylaspartate; NAAG, N-acetyl-aspartyl-glutamate; NFATc1, transcriptional activator of PSME; NSCLC, non-small cell lung cancers; PCa, prostate cancer; PLA, polylactic acid; PSA, prostate specific antigen; PSME, PSMA/GCPII enhancer; QD, quantum dots; RFC, reduced folate carriers; RIT, radioimmunotherapy; RNAi, RNA interference; SCLC, small cell lung cancer; Tfr, transferrin receptor

DOI:10.1111/bph.13576

Tables of Links

TARGETS	
Enzymes[a]	**G protein-coupled receptors**[c]
Folate hydrolase (prostate-specific membrane antigen) 1	mGlu3 receptor
Kallikrein related peptidase 3	**Transporters**[d]
Catalytic Receptors[b]	Reduced folate transporter 1, SLC19A1
Epidermal growth factor receptor	NIS, sodium iodide symporter
Fibroblast growth factor receptor 1	**Nuclear hormone receptors**[e]
Type I receptor serine/threonine kinases	AR, androgen receptor

LIGANDS	
DHT, dihydrotestosterone	Insulin-like growth factor 1
EGF	L-glutamic acid
GnRH I	Matrix metalloproteinase 2
IL-6	NAAG, N-acetyl-aspartyl-glutamate

These Tables list key protein targets and ligands in this article which are hyperlinked to corresponding entries in http://www.guidetopharmacology.org, the common portal for data from the IUPHAR/BPS Guide to PHARMACOLOGY (Southan *et al.,* 2016), and are permanently archived in the Concise Guide to PHARMACOLOGY 2015/16 ([a,b,c,d,e]Alexander *et al.,* 2015a,b,c,d,e).

Introduction

Prostate specific membrane antigen (PSMA) also known as glutamate carboxypeptidase II (GCPII), N-acetyl-L-aspartyl-L-glutamate peptidase I (NAALADase I) or N-acetyl-aspartyl-glutamate (NAAG) peptidase, is an enzyme that is encoded by the folate hydrolase (FOLH1) gene in humans (O'Keefe *et al.,* 1998). PSMA/GCPII plays many different roles and is expressed in different tissues such as the prostate, kidney, small intestine, central and peripheral nervous system and thus is recognized by different names. This review focuses on the biological role of PSMA/GCPII, with the main emphasis on prostate cancer (PCa) and neurological diseases. PSMA/GCPII's exact function in PCa is unknown; however, many studies have linked its role to tumour progression and carcinogenesis (Yao *et al.,* 2008). In the brain, PSMA/GCPII metabolizes the neurotransmitter NAAG. PSMA/GCPII has now been identified as a target for therapeutic interventions and diagnostics in various neurological disorders and in PCa (Bařinka *et al.,* 2012).

PSMA/GCPII was first characterized by the murine monoclonal antibody 7E11, derived from mice immunized with partially purified, cell membrane fractions, isolated from the human prostate adenocarcinoma (LNCap) cell line (Horoszewicz *et al.,* 1986). Immunohistochemical analysis revealed high expression of PSMA/GCPII in the epithelial cells of the prostate with an intense overexpression in the cancerous tissue, compared with normal or hyperplastic prostates. Other tissues have also shown to express lower amounts of PSMA/GCPII, for example epithelia of small bowel and the proximal tubules of the kidney (Chang *et al.,* 2000). PSMA/GCPII is encoded by a gene that consists of 19 exons, spanning 60 kilobases (Kb) of genomic DNA. The cDNA encoding PSMA/GCPII is 2.65 Kb in length and is mapped to chromosome 11 (Israeli *et al.,* 1993; O'Keefe *et al.,* 1998). It is a class II transmembrane glycoprotein, with a short N-terminal cytoplasmic tail of 1–18 amino acids (aa), a single membrane-spanning helix of 19–43 aa and an extracellular part, consisting of 44–750 aa with an approximate molecular weight of 84 kDa (Barinka *et al.,* 2004). The short N-terminal cytoplasmic tail interacts with membrane scaffold proteins that govern the endocytosis of some of the PSMA/GCPII bound substrates, such as clathrin, clathrin adaptor protein 2, filamin A (FLNa), and caveolin-1 (Anilkumar *et al.,* 2003; Rajasekaran *et al.,* 2003; Anilkumar *et al.,* 2006; Goodman *et al.,* 2007). The bulk of this transmembrane protein is the extracellular part, which is further divided in three domains, namely, the protease (57–116 aa and 352–590 aa), apical (117–351 aa) and the C-terminal domain or the dimerization domain (591–750 aa) and collectively performs the substrate/ligand recognition role (Davis *et al.,* 2005; Mesters *et al.,* 2006; Bařinka *et al.,* 2012) (Figure 1). The 3-dimensional extracellular structure of PSMA/GCPII closely resembles the transferrin receptor (Tfr) with 54% homology with Tfr and 60% with Tfr2 (Kawabata *et al.,* 1999; Lawrence *et al.,* 1999). This homology has been found both at the levels of aa (PSMA: 276–592 aa and Tfr: 316–606 aa) and domain organization (Mahadevan and Saldanha, 1999). In the small intestine, PSMA/GCPII is located in the brush border of the proximal jejunum, where it acts as a hydrolase on poly-γ-glutamated folate and actively transports the mono-glutamylated folates into the blood stream (Pinto *et al.,* 1996; Luthi-Carter *et al.,* 1998; Zhao *et al.,* 2009; Navrátil *et al.,* 2014). It thus exhibits both hydrolysing and endocytic functions. However, it is to be noted that PSMA/GCPII mediated poly-γ-glutamated folate hydrolysis is only observed in pigs and humans whereas, in rats, the same hydrolysing activity requires an intracellular enzyme called γ-glutamyl hydrolase FOLH1 that is abundant in the postprandial pancreatic secretion (Shafizadeh and Halsted, 2007). The endocytic internalization is through

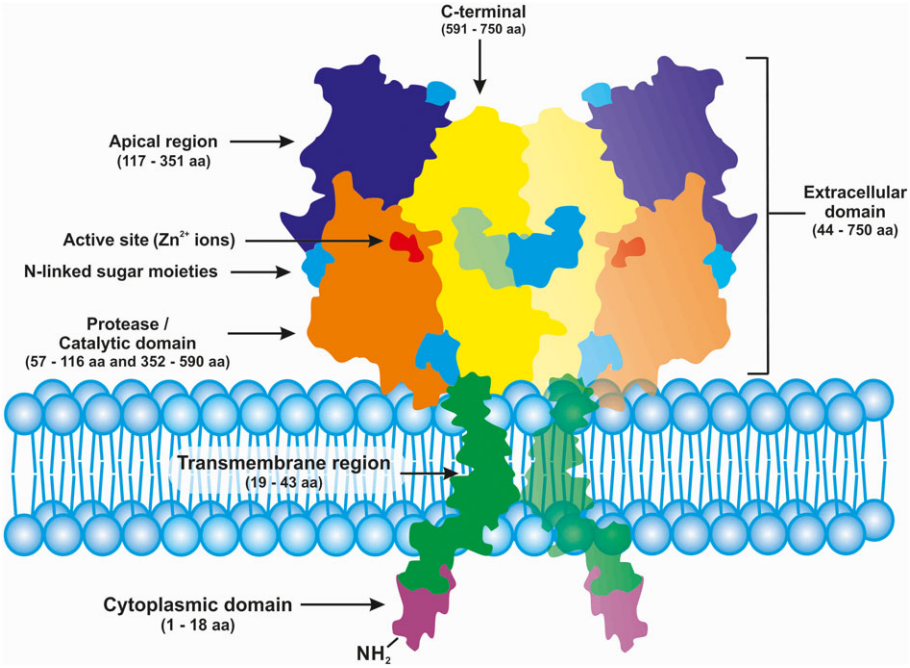

Figure 1

Schematic representation of PSMA/ GCPII transmembrane protein (homodimer). Adapted and modified from Bařinka *et al.,* (2012).

clathrin coated pits, which are specific for receptor-mediated endocytosis. In the nervous system, PSMA/GCPII, also termed as NAAG-Hydrolase, catalyses the hydrolysis of NAAG (a widely distributed neurotransmitter in the mammalian brain) to glutamate and N-acetylaspartate (NAA) (Robinson *et al.,* 1987; Coyle, 1997; Neale *et al.,* 2000).

The various roles of PSMA/GCPII in different tissues have enabled the exploration of various therapeutic approaches to target the delivery of drugs and small molecules specifically to PSMA/GCPII-expressing cells. As mentioned above, PSMA/GCPII expression levels are higher in the malignant tissues of different origin than the normal/healthy tissues (Chang *et al.,* 1999a,b; Milowsky *et al.,* 2007; Morris *et al.,* 2007; Haffner *et al.,* 2009). This directly implies a role of PSMA/GCPII in cancer progression and invasion (Conway *et al.,* 2006; Yao and Bacich, 2006; Yao *et al.,* 2010b). Thus, this makes PSMA/GCPII highly desirable for imaging and treatment of solid tumours or be used to develop targeted drug inhibitors that block its enzymatic activity.

Physiological function of PSMA/GCPII and its role in prostate cancer

In PCa, the expression of PSMA/GCPII is negatively regulated by androgens (Israeli *et al.,* 1993) and is favoured by other growth factors such as, basic fibroblast growth factor, TGF and EGF. The increased PSMA/GCPII expression in PCa tissues leads to an increased ability to process folate. However, the direct role of PSMA/GCPII in PCa metastasis is still unknown.

Prostate cancer involves a range of different molecules that participate in different signalling pathways. The prostate gland is regulated by the androgen hormone (testosterone), and this hormone plays an important role in the development and maintenance of the organ. The androgen-signalling axis is directly involved in PCa. Under normal circumstances, testosterone is converted to an active metabolite dihydrotestosterone (DHT) via 5-α reductase enzyme in the cytoplasm. DHT binds and activates the androgen receptor (AR), which translocates to the nucleus to bind its target gene and regulate gene expression (Zhou *et al.,* 1995; Wright *et al.,* 1996) (Figure 2). However, the AR can also be activated via insulin growth factor 1, EGF and IL-6 signalling pathways (Lonergan and Tindall, 2011). Targeting the androgen axis has now become the prime therapeutic target for PCa. Hormonal therapy, known as androgen ablation therapy, with luteinizing-hormone-releasing hormone agonists, is mostly used for advanced stages of the disease. However, this therapy fails after 18–24 months, indicated by rising prostate specific antigen (PSA) levels in the blood (Pienta and Bradley, 2006). The increased PSA levels along with the resurgence in the expression of AR-regulated genes lead to an aggressively malignant, metastatic and non-treatable type of PCa, called castration-resistant PCa. On the other hand, hormonal therapy on androgen sensitive cells has been shown to increase PSMA/GCPII levels. Interestingly, in this study, it was observed that the increased expression of PSMA/GCPII makes the cells less invasive in nature. This was indirectly confirmed by PSMA/GCPII knockdown (KD) in LNCap cells (which endogenously express PSMA/GCPII), which resulted in a five-fold increase in invasive activity (Ghosh *et al.,* 2005b). However, other studies have contradicted this finding and have shown that reduced expression of PSMA/GCPII

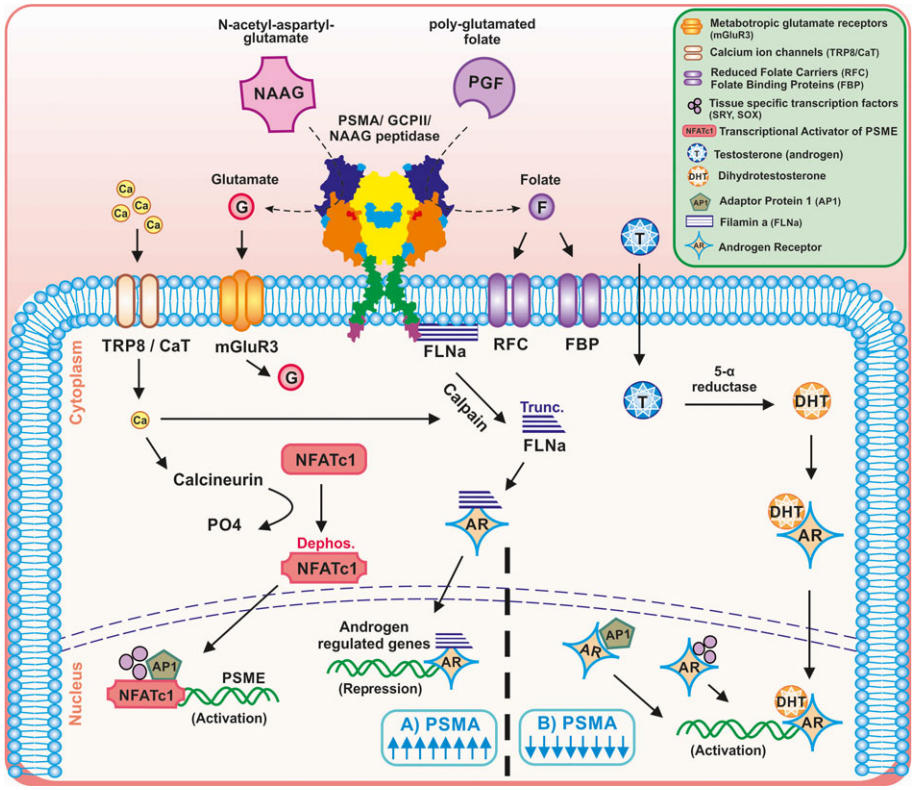

Figure 2

Schematic representation of PSMA/GCPII regulation in prostate cancer cells Adapted and modified from Ghosh and Heston (2005a). Up-regulation and down regulation of PSMA by Ca^{2+} ions and AR, respectively, is shown. (A) PSMA upregulation: NAAG and polyglutamated folates (PGF) are enzymically cleaved to folates and glutamates. The folates are taken up by the RFC or FBP present on the cell membrane. The glutamates activate the metabotropic glutamate receptors, which on activation, lead to the efflux of Cl^- ions and influx of Ca^{2+} ions. Ca^{2+} ions further alter the expression of PSMA in two ways. First by activating the inactive transcription factor NFATc1 (which is a transcriptional activator of PSMA enhancer [PSME]), or cause activation of calpain, which cleaves FLNa. The truncated FLNa binds to AR and localizes to the nucleus and suppresses AR-mediated transactivation. This effect leads to the upregulation of PSMA expression. (B) PSMA downregulation. Under normal conditions the cells do not express PSMA. Testosterone, an androgen is taken up by cells and is converted by 5-α reductase enzyme to the active metabolite DHT. AR binds to the DHT and translocates it to the nucleus, where they activate the androgen-regulated gene, thus down regulating PSMA expression. AR would also interact and sequester the transcription factor AP1 or tissue-specific transcription factors, such as, SRY and SOX, which suppress the transcription of PSME.

leads to reduction in invasiveness (Guo *et al.*, 2011; Conway *et al.*, 2013).

A possible signalling pathway that leads to increased expression of PSMA/GCPII in PCa cells has been shown to be regulated by the PSMA/GCPII enhancer (PSME) (1.2 Kb, located within the third intron of FOLH1) (O'Keefe *et al.*, 2000; Watt *et al.*, 2001). As mentioned before, PSMA/GCPII expression is negatively regulated by androgen, but it is also positively regulated by Ca^{2+} ions. The enzymatic activity of PSMA/GCPII hydrolyses the polyglutamated folates into folates and glutamates. The folates are internalized by the cells via reduced folate carriers (RFC) and folate-binding proteins (FBP). The released glutamates bind and activate the metabotropic glutamate mGlu3receptors, leading to efflux of Cl^- and influx of Ca^{2+} ions, via a CaT-like calcium channel (Shuba *et al.*, 2000; Wissenbach *et al.*, 2001). The influx of Ca^{2+} further modulates the expression of PSMA/GCPII by two pathways. The first is by activating the transcriptional activator of PSME (NFATc1). The NFATc1 protein undergoes dephosphorylation via calcineurin and is translocated to the nucleus and activates transcription of PSMA/GCPII. The second pathway is by activating calpain, which cleaves FLNa (a membrane scaffold protein, which facilitates internalization of substrates bound to PSMA/GCPII). Cleaved FLNa binds to the AR and localizes to the nucleus and suppresses AR-mediated transactivation. Under normal circumstances, AR would repress PSME by binding to AP1 or tissue specific transcription factors, such as SRY and SOX in the nucleus, which would explain why PSMA/GCPII levels are negatively regulated by androgens (Figure 2) (Ghosh and Heston, 2005a).

In PCa, the degree of PSMA/GCPII expression is positively correlated with the Gleason score and disease progression (i.e. the more advanced the stage of the disease, the greater the level of PSMA/GCPII expression in the prostate tissue). In addition, the rapid internalization and recycling of this receptor means that high concentrations of a targeted drug can be accumulated in PSMA/GCPII positive cells (Behnam Azad *et al.*, 2015).

PC3 cells were transfected to express PSMA/GCPII. These cells showed a significant increase in proliferation levels when compared with non-transfected counterparts. This increase was attributed to the enzymatic activity of PSMA/GCPII, as the effect was reversed in the presence of a PSMA/GCPII enzyme inhibitor (Yao *et al.,* 2010a). Interestingly, PSMA/GCPII has been shown to be expressed in two AR-negative canine cell lines of PCa; Leo and Ace-1. Leo cells form brain metastases in a xenograft mouse model, while Ace-1 cells metastasise to the bone to form osteoblastic and osteolytic lesions that mimic human metastases (Wu *et al.,* 2014).

Many studies have assessed the role of PSMA/GCPII in the initiation, progression and metastasis of PCa cells. The effect of inhibiting PSMA/GCPII in PCa has been studied, using lentiviral delivery of PSMA/GCPII shRNA in the PSMA/GCPII positive cell line, LNCaP (Guo *et al.,* 2011). The results from this study indicated that reduced PSMA/GCPII expression suppressed cell growth, induced significant cell cycle arrest at G_0/G_1 and reduced invasiveness. It has further been hypothesised that this reduction in cell proliferation and invasion is due to the deactivation of the p38 MAPK pathway that was observed following PSMA/GCPII silencing (Zhang *et al.,* 2013). As well as the p38 MAPK pathway, the KD of PSMA/GCPII has been shown to down-regulate p-Akt in the P13K/Akt signalling pathway, and Akt has been proposed as a downstream effector gene of PSMA/GCPII (Guo *et al.,* 2013b).

Recently, a relationship has been established between matrix metalloproteinase 2 (MMP2) and PSMA/GCPII (Conway *et al.,* 2013). Increased MMP expression has been widely associated as a characteristic of tumour progression and metastasis (Evans *et al.,* 2015). Sequential proteolysis of laminin (a component of the extracellular matrix) by MMP2 and PSMA/GCPII produced small peptide fragments that increased the rate of endothelial cell migration. This two-step degradation pathway highlights the possible role that PSMA/GCPII activation has on the induction of angiogenesis and metastasis (Conway *et al.,* 2013).

PSMA/GCPII in other cancers

In a study of 92 patients with invasive breast cancer, 98% had PSMA/GCPII staining that was confined to the neovasculature of the tumour. In all of the cases examined, normal breast tissue as well as carcinoma cells were PSMA/GCPII negative. In the same study, the level of PSMA/GCPII expression in 14 patients with brain metastases as a result of breast cancer was also determined. All 14 samples stained strongly for PSMA/GCPII, and interestingly, ten of the brain metastasis patients had a similar PSMA/GCPII staining score to their respective primary breast carcinoma (Wernicke *et al.,* 2014).

Samples from 150 lung cancer patient samples were examined for the presence of PSMA/GCPII in the tumour cells and surrounding neovasculature (Wang *et al.,* 2015). Approximately 85% of non-small cell lung cancers (NSCLC) and 70% of small cell lung cancer (SCLC) samples showed PSMA/GCPII expression in the neovasculature but was absent from normal blood vessels. Interestingly, while there was strong PSMA/GCPII staining within the tumour cells of NSCLC (over 50% of samples exhibited staining), this was absent from the SCLC tumours. It is not surprising that the PSMA/GCPII expression differs between these cancer types as they have their own unique biology and genetic aberrations (Oser *et al.,* 2015).

Evaluation of PSMA/GCPII expression in patients with colorectal cancer revealed two interesting correlations. There were positive relationships between PSMA/GCPII expression and metastasis to distant sites as well as to invasion of surrounding vasculature (Abdel-Hadi *et al.,* 2014). PSMA/GCPII mRNA expression levels are elevated in pancreatic adenocarcinomas compared with normal tissues. In this study, those patients with high expression of PSMA/GCPII had a significantly shorter overall survival than those with low expression levels, and PSMA/GCPII expression was shown to be correlated to Tumour-Node-Metastasis stage (Ren *et al.,* 2014).

In 167 bladder cancer patients of various subtypes (adenocarcinoma, small cell, urothelial and squamous cell), samples tested positive for PSMA/GCPII staining in the tumour neovasculature, with small cell tumour vasculature showing the greatest intensity. As with PSMA/GCPII expression in lung cancer samples, there were discrepancies in PSMA/GCPII staining within the tumour between the different cancer cell types (Samplaski *et al.,* 2011).

In a recent study, PSMA expression in four grades of glioma (astrocytoma) was determined. The surrounding vasculature of grade IV gliomas (glioblastoma multiforme) stained heavily for PSMA, while grades II and III showed little staining of the surrounding blood vessels but some staining of tumour parenchyma cells. The level of PSMA expression for grade IV tumours was three times greater than that seen in normal brain tissue (Nomura *et al.,* 2014).

Physiological function of PSMA/GCPII and its role in neurological diseases

In the brain, PSMA/GCPII acts as an enzyme and performs NAAG-hydrolyzing activity, as illustrated in Figure 3. Using Mab GCP-04, which binds the extracellular portion of PSMA/GCPII, approximately 50–300 ng of PSMA/GCPII per mg of total protein depending on the region was detected, with astrocytes showing GCPII expression in all parts of the brain (Šácha *et al.,* 2007). In astrocytes, the drug valproic acid increased the stability of GCPII due to the acetylation of lysine residues (Choi *et al.,* 2014).

According to Figure 3, NAAG is synthesized in neurons from glutamate and NAA with the help of NAAG-synthetase I and is stored in synaptic vesicles of presynaptic axon terminals (Williamson and Neale, 1988; Becker *et al.,* 2010; Neale *et al.,* 2011). A second structurally related protein, NAAG synthetase II has been discovered with similar NAAG synthesizing activity. The physiological role of this protein remains to be determined (Lodder-Gadaczek *et al.,* 2011). On depolarisation, NAAG is released from the synaptic vesicles into the extra-synaptic space, in a calcium-dependent manner. After being released, NAAG can interact with its target receptors, mainly the metabotropic glutamate mGlu3 receptor located on both presynaptic nerve terminals and astrocytes. The interaction with mGlu3 receptors leads to the signalling

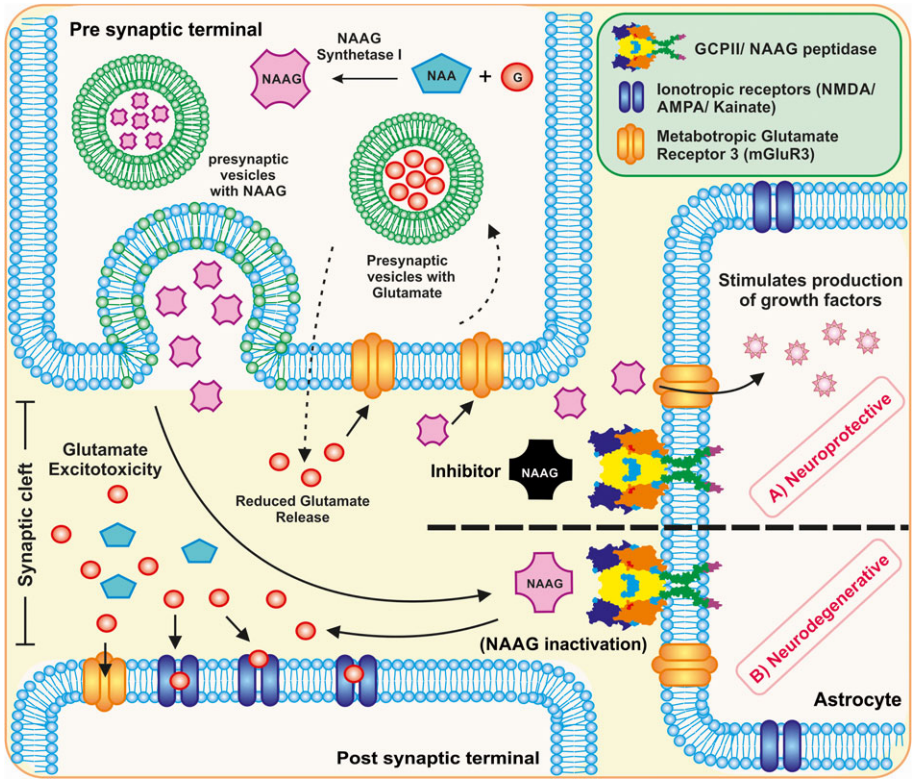

Figure 3

Schematic representation of the role of PSMA/GCPII in the brain. PSMA/GCPII is expressed on the astrocytes and can lead the cells towards a neurodegenerative or a neuroprotective outcome. (A) in the neuroprotective role, to reduce the glutamate excitotoxicity, NAAG inhibitors can be used to competitively bind to the PSMA or to the glutamate receptor, avoiding the hydrolysis of NAAG into NAA and glutamate. Due to this effect, NAAG interacts with the metabotropic receptors on astrocytes, which leads to the production of growth factors and thus acts as a neuroprotective agent. NAAG and glutamate are also regularly recycled into the presynaptic neuron via G-protein coupled pathway and glutamate-glutamine pathway, respectively. (B) in the neurodegenerative role, NAAG, a neuropeptide released from the presynaptic neuron in the brain interacts with the PSMA/GCPII transmembrane protein. The interaction causes hydrolysis of NAAG into NAA and glutamate. The excess of glutamate leads to glutamate excitotoxicity in the synaptic cleft and further activates the ionotropic and metabotropic receptors on the post synaptic terminal of the neuron, leading to degeneration of cells.

of G-protein coupled pathway, resulting in the reduced release of neurotransmitters such as GABA from pre-synaptic nerve terminals (Zhao *et al.,* 2001; Sanabria *et al.,* 2004; Zhong *et al.,* 2006; Romei *et al.,* 2013). At the astrocyte level, the NAAG and mGlu3 receptor interaction stimulates the secretion of TGFs and peptides (Bruno *et al.,* 1998; Thomas *et al.,* 2001). Thus, the interaction of NAAG with mGlu3 receptors on either presynaptic nerve terminals or astrocytes are both considered to be neuroprotective in nature (Slusher *et al.,* 1999; Gurkoff *et al.,* 2013; Cao *et al.,* 2016). Another fate of NAAG in the extra-synaptic space involves the inactivation of NAAG in the presence of PSMA/GCPII (NAAG peptidase) into NAA and glutamate and the reaction products are transported to astrocytes and oligodendrocytes (Riveros and Orrego, 1984). About 80–90% of the glutamate in the neurons is recycled via the glutamate-glutamine cycle and thus a regulated recycling of glutamate maintains the healthy functioning of the brain.

Decades of research has shown that in order to be effective at inhibiting PSMA/GCPII activity, potential compounds must meet two criteria: a glutarate moiety to bind the glutamate recognition site and a zinc chelating group for the zinc atoms at the PSMA/GCPII active site (Bařinka *et al.,* 2012). At present, there are several classes of PSMA/GCPII inhibitor, which are phosphonate-based, urea-based, thiol-based and also hydroxamate derivatives (Tsukamoto *et al.,* 2007; Bařinka *et al.,* 2012; Ferraris *et al.,* 2012). It is important to note that these inhibitors do not have an effect on glutamate function at normal levels of activity (Slusher *et al.,* 1999).

One of the first successful inhibitors of GCPII, 2-(phosphonomethyl)pentanedioic acid (2-PMPA), a phosphonate analogue of glutamate, was designed in 1996 and is extremely potent, with an IC_{50} of 300 pM (Jackson *et al.,* 1996). 2-PMPA (NAALADase inhibitor) has shown efficacy in inhibiting PSMA/GCPII activity in over 20 various *in vivo* models of neurological disease, including schizophrenia, ischemic brain injury and neuropathic pain (Table 1). Unfortunately, 2-PMPA has exhibited poor pharmacokinetics due to its highly polar nature, which has led to structure–activity relationship studies, yielding more potent inhibitors, such as GPI5232 and VA-033 (Zhong *et al.,* 2014). In a recent study, 2-PMPA was administered to the brain intranasally in non-human primates and, 30 min later, the level of 2-PMPA was below the limit of detection in the

Table 1

List of GPCII/NAALADase inhibitor (2-PMPA) studies focussing on neurological disorders

Neurological disorder	Dose	Route	Animal model	End-point comments	References
Neuropathic pain	50 and 100 mg·kg^{-1}	IV	Sprague–Dawley rats	Significant increase in paw-withdraw threshold in rats with partial ligation of the left from less than 5 g at 45 min to ~14 g and 19 g, respectively. Significant decrease in the spontaneous ectopic discharges recorded from injured sciatic afferent nerves from ~15 imp.·s^{-1} for the control group to ~10 imp.·s^{-1} and ~5 imp.·s^{-1}, respectively, for treatment groups Significant improved allodynia induced by sciatic nerve ligation	(Chen *et al.*, 2002)
Chronic pain	50 mg·kg^{-1}	IP	Wistar rats/ Sprague–dawley rats	After 2-PMPA dose administration, the maximum concentration achieved in brain ECF was 30 μM. Following 2-PMPA administration, a steady increase of NAAG in brain ECF was observed, reaching a peak concentration of 3 μM. The study concludes that the low concentration of NAAG in the brain ECF is unlikely to have an effect on any known target, and so they say that the effect of inhibitor is unlikely to be mediated by either NAAG or mGluR3.	(Nagel *et al.*, 2006)
Diabetic neuropathy	n/a	n/a	n/a	2-PMPA rescued the dorsal root ganglion neurons from glucose induced programmed cell death mGluR3 antagonist EGLU reversed the 2-PMPA protection profile in three assays testing for apoptosis; caspase-3 and −9 cleavage, and TUNEL This reversal was not seen with either the group I mGluR antagonist AIDA, nor the group 3 mGluR antagonist MSOP. At high glucose concentrations, 2-PMPA was able to maintain neurite growth and viability.	(Berent-Spillson *et al.*, 2004)
Inflammatory pain	100 μg	IT	Sprague–Dawley rats	In the rat formalin test (model for inflammatory pain), 2-PMPA attenuated the phase 1 and 2 biphasic flinching when rats were pre-treated with inhibitor prior to the formalin test. In the post-treatment test, 2-PMPA had no effect on biphasic flinching. 2-PMPA did not have an effect on the reaction time of the rats in the hot plate test	(Yamamoto *et al.*, 2001b)
Inflammatory pain	10 μg	ICV	Sprague–Dawley rats	Significant reduction in the phase 1 and 2 biphasic flinching in the rat formalin test with 2-PMPA. These effects were attenuated following the administration of group II mGluR antagonist LY341495	(Yamamoto *et al.*, 2008)
Pain	100–400 μg	IT	Sprague–Dawley rats	2-PMPA improved the level of allodynia induced by paw carrageenan injection. However, this improvement was not observed for other models of pain (i.e. skin incision or mild thermal injury.)	(Yamamoto *et al.*, 2001a)
Peripheral pain	1–100 μg	SC	Sprague–Dawley rats	Group II mGluR agonists (SL_X-3095-1 and APDC) and 2-PMPA reduced the pain response in the rat formalin test.	(Yamamoto *et al.*, 2007)

continues

Table 1 (Continued)

Neurological disorder	Dose	Route	Animal model	End-point comments	References
				Group II mGluR agonists (SL_X-3095-1, NAAG and APDC) and 2-PMPA reduced the pain response in the carrageenan model of induced allodynia These effects were attenuated following the administration of group II mGluR antagonist LY341495	
Brain injury from soman	50 mg·kg^{-1}	IP	Sprague–Dawley rats	The nerve agent soman was shown to reduce NAAG levels in regions of the brain following exposure The administration of 2-PMPA reduced neuronal cell death in some (but not all) regions of the brain following exposure to soman; these regions include the entorhinal cortex, piriform cortex and the amygdala	(Guo *et al.*, 2015)
Spinal cord injury	1–4 μM	subarachnoid space	Sprague–Dawley rats	The co-administration of somatostatin with 2-PMPA and dynorphin A (causes ischemic spinal cord injury) along with 2-PMPA as a spinal subarachnoid injection resulted in improved hindlimb motor scores by 24 h post injection. Significant reduction of the extracellular concentrations of glutamate in cerebrospinal fluid was observed when 2-PMPA was co-administered with dynorphin A, in comparison to mice treated with dynorphin A alone	(Long *et al.*, 2005)
Ketamine-induced neurotoxicity	n/a	n/a	n/a	2-PMPA attenuated the decrease in cell viability seen with 2 mM of ketamine in neuron–glia mixed culture by decreasing the loss of nodes/cell from $<$0.5 with 50 μM of 2-PMPA to $>$1.00 with 100 μM of 2-PMPA but the same effect was not observed in cultures of neurons alone. The authors conclude that glia cells must be involved in the neuroprotective effect that 2-PMPA offers.	(Zuo *et al.*, 2014)
Neurotoxicity	n/a	n/a	n/a	The degree of neuroprotection offered by 2-PMPA in an *in vitro* model of primary neurons (neurotoxicity) from rat embryos was 100%, 46%, 16% and 0% for hypoxia, glutamate, NMDA injury and veratridine-induced injury	(Tortella *et al.*, 2000)
Alcohol	50, 100 and 200 mg·kg^{-1}	IP	Alcohol preferring P rat	Significant reduction in the consumption of ethanol by alcohol preferring rats by ~25% during their daily 1-hour access to 10% (*v*/v) ethanol following treatment with 2-PMPA	(McKinzie *et al.*, 2000)
Cocaine	0.01–100 μM	Local exposure	Planarians (*Dugesia dorotocephala*)	2-PMPA attenuated the C-like hyperkinesias (i.e., stereotypical counts) induced in planarians by four compounds; glutamate, NMDA, pilocarpine and cocaine	(Tallarida *et al.*, 2012)
Cocaine	100 mg·kg^{-1} and 30 mg·kg^{-1}	IP / PO	Sprague–Dawley rats	The acquisition of the conditioned place preference (CPP) response was blocked by either 100 mg·kg^{-1} 2-PMPA i.p. or 30 mg·kg^{-1} p.o. of GPI 5693; an orally bioavailable NAALADase inhibitor. Administration of either drug in the absence of cocaine did not significantly alter the time spent in each chamber. 2-PMPA did not significantly reduce the CPP response that has been shown to be induced by food.	(Slusher *et al.*, 2001)

continues

Table 1 (Continued)

Neurological disorder	Dose	Route	Animal model	End-point comments	References
Cocaine	10, 30 and 100 mg·kg^{-1}	IP	Long-Evans rats	Inhibition of intravenous self-administration of cocaine. Dose-dependent reduction in extracellular dopamine and glutamate after 2-PMPA administration. Successful prevention of cocaine-induced reinstatement of drug-seeking behaviour	(Xi *et al.*, 2010b)
Cocaine	1, 10, 30 and 100 mg·kg^{-1}	IP	Long-Evans rats	Significant inhibition of cocaine self-administration under progressive-ratio (PR) reinforcement conditions Significant inhibition of cocaine-enhanced brain-stimulation reward (BSR) in rats. Dose-dependent reduction in cocaine-induced extracellular dopamine in the nucleus accumbens (NAc).	(Xi *et al.*, 2010a)
Cocaine	100 mg·kg^{-1}	IP	Sprague–Dawley rats	Increased locomotor activity of the rats following 2-PMPA administration No significant difference in the distance travelled between the control (saline) and the mice pre-treated with 2-PMPA, following cocaine administration after 15 min 2-PMPA prevents the sensitization that develops to the locomotor activity, following cocaine use.	(Shippenberg *et al.*, 2000)
Cocaine-kindled seizures	10, 30 and 100 mg·kg^{-1}	IP	Swiss-Webster mice	2-PMPA was shown to prevent the expression and development of cocaine kindling. Mice pretreated with 2-PMPA showed a lower % of mice convulsing when challenged with 60 mg·kg^{-1} of cocaine following 10 days of treatment with 40 mg·kg^{-1} of cocaine. The inhibitor dose did not alter the behaviour of the mice in the inverted screen test and locomotor activity.	(Witkin *et al.*, 2002)
Ischemic brain injury	500 mg·kg^{-1}	IV	Sprague–Dawley rats	Reduction in the extent of injury (magnitude of protection was 54%) in an established focal ischemia model. Using microdialysis, it was shown that the levels of glutamate in the mice treated with inhibitor showed no increase following middle cerebral artery occlusion (MCAO). In non-ischemic mice, the inhibitor did not alter basal levels of glutamate	(Jackson *et al.*, 1996)
Ischemic strokes	n/a	n/a	n/a	Ischemic strokes result in an increase in the extracellular concentration of glutamate, which tends to overactivate the *N*-methyl-D-aspartate receptors (NMDARs) The inhibitor was shown to increase the amplitude of the synaptic NMDAR excitatory postsynaptic currents (EPSCs) while decreasing the extrasynaptic NMDAR ESPCs.	(Khacho *et al.*, 2015)

continues

Table 1 (Continued)

Neurological disorder	Dose	Route	Animal model	End-point comments	References
Schizophrenia	50–150 mg·kg^{-1}	IP	C57BL/6 and DBA/2 mice	Group II agonist LY354740 was able to moderate the effects of PCP on prepulse inhibition (PPI) of acoustic startle in DBA/2 but not C57BL/6 mice 2-PMPA was unable to affect the PCP-mediated PPI in either strain.	(Profaci *et al.*, 2011)
Schizophrenia	100 mg·kg^{-1}	IP	C57BL/6 mice, DBA/2 mice and Sprague–Dawley rats	2-PMPA reduced the motor activation in PCP or *d*-amphetamine induced models of schizophrenia These effects were not observed in mice that are homozygous for a deletion in GCPII 2-PMPA attenuated the effect of dizocilpine (MK-801) in an object recognition test; a model for the cognitive impairment seen in schizophrenia	(Olszewski *et al.*, 2012)
Memory Process	150 mg·kg^{-1}	IP	Swiss-Webster mice	No negative impact of the dose on long term memory in the passive avoidance task. Increased latency to enter the dark box on training day from ~24 s in control mice to ~103 s in treated mice. The dose impaired spontaneous alternation in the Y-maze task. NAALADase inhibition may impair alternation behaviour	(Łukawski *et al.*, 2008)
Memory Process	0.2–100 mg·kg^{-1}	IP	C57BL/6 mice	In comparison to the control mice, the mice treated with 2-PMPA spent significantly more time exploring the novel object compared with the familiar object on day two. Mice that were homozygous for a deletion in GCPII displayed the same results as those treated with the inhibitors.	(Janczura *et al.*, 2013)
Neurodegenerative disorders	30 mg·kg^{-1} for each dose	IN/IP	Wistar rats, Cynomolgus monkey	i.n. administration showed higher levels of 2-PMPA accumulation in olfactory bulb and the cerebellum compared with i.p. administration, but had similar plasma profiles. In a non-human primate study, 2-PMPA achieved micromolar concentrations following i.n. delivery.	(Rais *et al.*, 2015)

plasma (<50 nM), but reached 1.5 μM in the cerebrospinal fluid. This study highlights a direct pathway for delivering 2-PMPA to the CNS via the olfactory nerve (Rais *et al.*, 2015).

In an attempt to reduce the highly polar nature of the phosphonate-based inhibitors, researchers substituted the phosphorus group with thiol, leading to the design of 2-(3-mercaptopropyl) pentanedioic acid (2-MPPA) (Majer *et al.*, 2003). 2-MPPA was the first orally bioavailable PSMA/GCPII inhibitor with studies conducted in humans (Majer *et al.*, 2003; Van der Post *et al.*, 2005). Similar to 2-PMPA, 2-MPPA exhibited efficacy in a range of animal models of neurological disease, including neuropathic pain, neuropathy and ALS (Ghadge *et al.*, 2003; Potter *et al.*, 2014). Although, no adverse CNS effects were reported, further studies were halted as a result of the potential for immune toxicity, common with thiol-containing drugs, as well as a relatively low therapeutic potency (Bařinka *et al.*, 2012).

A further class of PSMA/GCPII inhibitors comprises the urea-based inhibitors (Kozikowski *et al.*, 2001). These inhibitors were initially developed by medicinal chemist Alan Kozikowski from the NAAG-based mimic 4,4′-phosphinicobis (butane-1,3-dicarboxylic acid) (Nan *et al.*, 2000). ZJ43 is a well-studied urea-based analogue developed by this group that reduced PCP-induced motor activation in a rodent model of schizophrenia (Olszewski *et al.*, 2004). In the rat formalin test of neuropathic pain, IV administration of ZJ43 suppressed both phases of agitated behaviour and attenuated allodynia following sciatic nerve ligation (Yamamoto *et al.*, 2004). In a rat model of traumatic brain injury, ZJ43 significantly reduced the number of ipsilateral degenerating neurons and significantly reduced ipsilateral astrocyte loss (Zhong *et al.*, 2005). There are several advantages to using urea-based inhibitors including ease of their synthesis as well as subsequent modification and conjugation (Ferraris *et al.*, 2012). Molecules based on these early stage urea-based prototypes have been conjugated to various imaging agents and therapeutic payloads to diagnose and treat PCa at the preclinical stage (Tables 2–4). However, in terms of treating neurological disorders, these molecules exhibit poor pharmacokinetics, as they tend to have low oral bioavailability and are very limited in their ability to cross the blood–brain barrier (BBB) due to their hydrophilic nature (Zhong *et al.*, 2014).

The closest homologue to PSMA/GCPII is glutamate carboxypeptidase III (GCPIII) (Hlouchová *et al.*, 2007). While investigating closely related peptidases, it was shown that GCPIII has a similar NAAG hydrolysing activity to PSMA/GCPII (Pangalos *et al.*, 1999). Despite these similar functions, GCPIII has several different motifs in the active site which account for the differing substrate specificities and inhibitor susceptibilities (Hlouchová *et al.*, 2007). In addition, GCPIII has recently been shown to have its own distinct function in the cleavage of β-citrylglutamate (Navrátil *et al.*, 2016).

Targeting PSMA/GCPII as a potential therapeutic approach

Chemotherapy

Traditional chemotherapies work against rapidly dividing cells (such as cancer cells). However, they also attack healthy cells of the body that naturally rapidly divide, such as those of the digestive tract or hair follicles (Sutradhar and Amin, 2014). Targeting chemotherapies to diseased tissues overexpressing a certain receptor (such as PSMA/GCPII) allows for minimal toxicity to normal tissue, while simultaneously allowing the drug to accumulate at a much higher concentration in the tumour tissue compared with the free drug (Sun *et al.*, 2014b; Pérez-Herrero and Fernández-Medarde, 2015). There are numerous studies that exploit the PSMA/GCPII for targeted delivery of chemotherapeutic drugs in PCa, either via aptamers, antibodies or small molecules (Table 2).

A PSMA/GCPII-targeted generation 5 PAMAM dendrimer has been used to deliver methotrexate (Huang *et al.*, 2014). A urea-based small molecule (glutamate urea) was used as a targeting ligand for PSMA/GCPII. The urea-based conjugate showed binding to LNCaP cells in a dose-dependent manner, in contrast to the control which did not yield any significant binding. The targeted conjugate also induced potent cytotoxicity in LNCaP cells, with no observable difference in PSMA/GCPII negative PC3 cells between control and targeted formulations.

Micelles have recently been developed with a H40 polymer core and an amphiphilic copolymer containing the hydrophobic polylactic acid (PLA) facing inside and the hydrophilic polyethylene glycol (PEG) facing outside. The aptamer A10 was covalently linked to the PEG on the outer surface and allows for effective PSMA/GCPII targeting (Xu *et al.*, 2013). Aptamers are nucleic acid ligands (either DNA or RNA) that fold into a specific conformation that confers specificity for the intended target site (Sun *et al.*, 2014a). Hydrophobic doxorubicin 'sits' in the PLA component of the micelle. Higher levels of doxorubicin were observed in the nucleus of CWR22Rv1 cells following treatment with the targeted formulations, while doxorubicin from the untargeted controls was mainly confined to the cytoplasm. In a CWR22Rv1 xenograft mouse model of PCa, the highest doxorubicin fluorescence intensity was observed in the tumours from the groups treated with targeted micelles (Xu *et al.*, 2013). Similarly, the small molecule PSMA/GCPII inhibitor was conjugated to PCL-PEG copolymers to form self-assembling micelles with the chemotherapeutic agent docetaxel in the core of the formulation. In this case, the targeted therapy had a lower IC_{50} and a five-fold higher increase in uptake compared with the non-targeted therapy (Jin *et al.*, 2014).

Aside from aptamers and small molecules, antibodies have also been used to target therapies to PSMA/GCPII positive cells (Wang *et al.*, 2011; Yallapu *et al.*, 2014; DiPippo *et al.*, 2015; Hariri *et al.*, 2015). Monomethylauristatin E was conjugated to a fully human anti-PSMA/GCPII antibody to form an antibody-drug conjugate (ADC) (Wang *et al.*, 2011). ADCs have shown significant clinical activity in patients that have been previously treated with chemotherapy (Krop *et al.*, 2010). Using this PSMA/GCPII ADC, the induction of cell death was shown to be 1000-fold higher in PSMA/GCPII positive cells. Also, in a docetaxel-resistant mouse model of PCa, the mean tumour volume was significantly lower in the PSMA/GCPII ADC group then when compared with docetaxel alone, with survival times significantly increased in the former group (Wang *et al.*, 2011).

Table 2

List of PSMA based therapeutics developed with focus on Chemotherapy and Gene therapy

Therapeutic payload	Delivery vector	Targeting ligand	*In vitro* model	*In vivo* model	Concluding remarks	References
Chemotherapy						
Methotrexate	PAMAM dendrimer	Glutamate urea	LnCap, PC3 cells	N/A	Nanoparticle binding and uptake observed in LnCap cells (PSMA+) and not in PC3 cells (PSMA-).	(Huang *et al.*, 2014)
CpG and Doxorubicin	Dendrimer	DNA-A9 PSMA (RNA aptamer hybrid)	RAW264.7, LNCaP, 22RV1, DU145, and PC3 cells	BALB/c mice (22RV1 xenograft tumour model)	Seventy-eight per cent decrease in tumour volume observed in animals treated with targeted nanoparticles compared with controls.	(Lee *et al.*, 2011)
Mono methylauristatin E	N/A	PSMA Monoclonal antibody	LNCaP, C4–2, CWR22rv1, and PC3, DU145, MDA PCa2b cells	Athymic nude mice (C4–2 xenograft tumour model)	1000-fold better cell death observed in cells that expressed PSMA. Effective in treating tumours in a C4–2 xenograft model that had progressed following treatment with docetaxel.	(Wang *et al.*, 2011)
Mono methylauristatin E	N/A	PSMA monoclonal antibody	LuCap 96CR PDM model	SCID mice	Complete tumour regression in LuCaP 96 CR xenograft mouse model, when treated with drug-antibody conjugate. The PDX model displayed a high level of PSMA expression.	(DiPippo *et al.*, 2015)
Docetaxel	PLA–PEG/ PLGA-PEG	ACUPA (small molecule)	N/A	Athymic nude mice (LnCap xenograft model) / Male Sprague–Dawley rats / Cynomolgus monkeys	Targeted nanoparticles had increased tumour accumulation and suppressed tumour growth in tumour bearing mice.	(Hrkach *et al.*, 2012)
Epirubicin	PEG	RNA aptamer (A10)	PC3 and LnCap cells	N/A	Reduced toxicity observed in PSMA- cell line when treated with PEG-Apt-Epi formulation versus Epirubicin alone. No difference in cell viability observed in PSMA+ cell line, when treated with epirubicin alone or PEG-Apt-Epi	(Taghdisi *et al.*, 2013)
Doxorubicin	PLA–PEG micelles	RNA aptamer (A10)	CWR22Rv1 cells	Athymic nude mice (CWR22Rv1 cells xenograft model)	Doxorubicin-loaded micelles showed increased uptake in PSMA+ 22Rv1 cells via PSMA-mediated endocytosis.	(Xu *et al.*, 2013)
Doxorubicin	Liposome	RNA aptamer	LnCap and PC3 cells	BALB/c athymic nude mice (LnCap xenograft model)	Targeted liposomes containing docetaxel were significantly more toxic to PSMA + cell line (LNCaP) than compared with PC-3 cell line (PSMA -) and also showed significant tumour regression in comparison untargeted liposomes or drug alone.	(Baek *et al.*, 2014)

continues

Table 2 (Continued)

Therapeutic payload	Delivery vector	Targeting ligand	*In vitro* model	*In vivo* model	Concluding remarks	References
Circumin	PLGA/PLL/PVA	PSMA antibody	LnCap, DU145, PC3 and C4–2 cells	Athymic nude mice	PSMA antibody tagged PLGA curcumin nanoparticles showed specific targeting in C4–2 cells (PSMA +) in a xenograft mouse model	(Yallapu *et al.*, 2014)
Indenoisoquinoline topoisomerase I inhibitor	N/A	DUPA	22RV1 cells	Athymic nude mice (22RV1 cells xenograft model)	After 40 days, complete regression of tumour growth was observed in the animals treated with DUPA-drug conjugate. DUPA conjugate exibited PSMA receptor-mediated uptake.	(Roy *et al.*, 2015)
Toremifene	PLGA-PEG nanoparticles	PSMA antibody	PC3M cells	Athymic nude mice	Incorporation of oestrogen receptor-α (ERα) blocker, toremifene, into PLGA nanoparticle resulted in a 15-fold increase in its uptake when compared with free toremifene. The model used was modified PC-3 cells to express PSMA (PC3M) orthotopically implanted into mouse prostate.	(Hariri *et al.*, 2015)
Doxorubicin	PEGylated PLA nanoparticle	RNA aptamer (A10)	LNCaP and PC-3 cells and canine prostatic adenocarcinoma cell line (cHSA) cell line	BALB/c mice	Mice treated with aptamer-conjugate showed a twofold increase in the amount of necrotic tissue in the tumour compared with the non-targeted nanoparticles. A significant reduction in tumour burden in the aptamer group after 7 days (~70%) was observed, when compared with the non-targeted group (14% reduction).	(Tang *et al.*, 2015)
Docetaxel	HPMA co polymer	DUPA	C4–2 and PC3 cell line	Athymic nude mice (C4–2 xenograft model)	Lower IC50 of targeted nanoparticles with DTX (3.18 ± 0.42 nM) compared with untargeted counterparts (4.14 ± 1.03 nM). Significantly ($p < 0.05$) reduction in tumour volume with targeted nanoparticles vs. untargeted nanoparticles (<800 mm^3 vs. >1500 mm^3 at 42 days post injection, respectively).	(Peng *et al.*, 2013)
Thapsigargin	Drug conjugated with peptide (Asp-Glu-Glu-Glu-Glu-Glu)	N/A	LNCaP, MDA-PCa2b, TSU, SN12C, and MCF-7 cells, CWR22R-H xenograft	Nude mice (Harlan Sprague Dawley)	This delivery vector takes advantage of the glutamate carboxypeptidase activity of PSMA to cleave the glutamate residues from the peptide to form 8-O-(12-aminododecanoyl)-8-O-debutanoyl thapsigargin (12ADT)-βAsp. This prodrug is over 60-fold more toxic to PMSA + cells than PSMA – cells. Delivery of thapsigargin in the prodrug form is 150-fold more effective than free thapsigargin.	(Denmeade *et al.*, 2012)

continues

Table 2 (Continued)

Therapeutic payload	Delivery vector	Targeting ligand	*In vitro* model	*In vivo* model	Concluding remarks	References
					Tumour regression and growth inhibition was observed in six *in vivo* tumour xenograft models with the prodrug.	
Suicide enzyme yCD	N/A	N/A	LnCap and PC3 cells	N/A	Significant reduction of cell viability in PSMA+ cell lines (~ 60% reduction), in comparison to PSMA- cell line (PC3)	(Martin *et al.*, 2014)
RNA aptamer A9 g	N/A	RNA apatmer A9 g	CT26, PC3 (PSMA +/−) and 22Rv1	SCID mice	A9 g binds and inhibits the enzymatic activity of PSMA. *A9 g demonstrated the ability to reduce cell invasion (~ 75% reduction) and migration (~ 70% reduction) of prostate cancer cells engineered to express PSMA (PC-3)	(Dassie *et al.*, 2014)
P13k Inhibitor ZSTK474 and immunotoxin J591PE	N/A	N/A	LnCap, C4–2 and BT-549	BALB/c nude mice	The combination of the 2 drugs resulted in increased apoptosis and cell deaths in PSMA+ cell lines (LNCaP and C4–2) compared with PSMA- (BT549).	(Baiz *et al.*, 2013)
TGX-221	PEG-PCL micelles	RNA aptamer A10	PC3, DU145 and LnCap cells	BALB/c nude mice	TGX-221 is a selective inhibitor of the P13K p110β catalytic subunit. Micelles that were targeted to PSMA resulted in a significant increase in uptake of drug in PSMA+ cells.	(Zhao *et al.*, 2012)
TGX-221	PEG-PCL micelles	–	LAPC-4, LNCaP, C4–2 and 22RV1 cells	Nude mice (LAPC-4, LNCaP, C4–2 and 22RV1 cells used for xenograft models)	*Complete inhibition of tumour growth in four mouse xenograft models (LAPC-4, LNCaP, C4–2 and 22RV1). Induction of apoptosis and reduction of PSA levels by approximately 80% in the four models tested.	(Chen *et al.*, 2015)
Cisplatin	PLGA-b-PEG NPs	RNA apatmer	LnCap cells	Sprague Dawley rats and Swiss Albino mice, BALB/c mice	Achieved greater maximum tolerated dose (MTD) for cisplatin was greater when encapsulated in NP than for free cisplatin. Enhanced residence time in blood. Reduction in tumour growth at much lower platinum dose than than cisplatin.	(Dhar *et al.*, 2011)
Epigallocatechin 3-gallate (EGCG)	PLGA-PEG	DCL	LnCap cells and HUVEC cells	N/A	Significantly greater reductions in LNCaP cell viability when EGCG was complexed in targeted vs non-targeted NP.	(Sanna *et al.*, 2011)
Genetherapy						
siRNA targeting Notch1	Two fusion proteins and a	PSMA antibody	LnCap adn DU145 cells	BALB/c nude mice	Significant KD of Notch1 in LNCaP mouse xenograft model	(Su *et al.*, 2013)

continues

Table 2 (Continued)

Therapeutic payload	Delivery vector	Targeting ligand	*In vitro* model	*In vivo* model	Concluding remarks	References
	truncated protamine					
siRNA targeting choline kinase (ChK)	PLL-PEG-PEI	PSMA inhibitor	PC3 cells	SCID and BALB/c mice	Theranostic vector contains I^{111} for imaging, bacterial cytosine deaminase and siRNA targeting Chk. Specific uptake of targeted nanoparticles into PSMA+ PC3-PIP tumours was observed. Nanoparticles were well tolerated with no liver or kidney toxicity and no immune response.	(Chen *et al.*, 2012)
siRNA targeting PSMA	Lentivirus	N/A	LnCap, DU145 and HEK 293 T-cells	N/A	Suppressed growth, migration and invasion of PSMA+ LNCap and DU145 cell lines	(Guo *et al.*, 2011)
siRNA targeting mTOR	Lentivirus	N/A	RWPE1, LNCap, C4–2b and HEK293 cells	SCID mice (C4–2b xenografts)	Tumour growth was significantly retarded in SCID mice treated with LV-PSMA-shmTOR.	(Du *et al.*, 2013)
ShRNA targeting DNAPK	N/A	Aptamer A10–3	DU145, LnCap and PC3 cells	Athymic nude mice	25% reduction in DNAPK expression in human prostate tissue by immunostaining compared with control aptamers. 60% cell death in LNCaP cells treated with aptamer-targeted shRNA. Combination of A10–3-DNAPK and radiation treatment (6 Gy) resulted in a significant and extended tumour response in LNCaP tumours but not PC-3 tumours.	(Ni *et al.*, 2011)
MiR-15a and miR-16-1	PAMAM-PEG	Aptamer A10–3.2	PC3 AD LnCap cells	N/A	Targeted nanoparticles showed sixfold higher transfection efficiency in LNCaP cells (in relation to untargeted NP). Targeted nanoparticles also showed a 5.47 fold lower IC50 compared with non-targeted control in LNCaP cells *in vitro*.	(Wu *et al.*, 2011)
HSV-TK and connexin43 gene	PAMAM dendrimer	Folate	LnCap, PC3, NIH3T3, HepG2,	Nude mice	HSV-TK and connexion43 gene expression was driven by PSMA promoter. Expression of these genes was confined to LNCaP cells (but absent from PC-3 cells).	(Chen *et al.*, 2013)
Bcl-xL shRNA (in combination with docetaxel)	PEI-PEG	Aptamer	LnCap cells	N/A	Three-fold higher transfection efficiency in LnCap cells with targeted nanoparticles.	(Kim *et al.*, 2010)

continues

Table 2 (Continued)

Therapeutic payload	Delivery vector	Targeting ligand	*In vitro* model	*In vivo* model	Concluding remarks	References
					LNCaP cell viability fell from 81% to 21% 48 h after treatment with NPs, with virtually no toxicity in PC-3 cells observed. IC_{50} value for the NPs loaded with docetaxel + shRNA was 17-fold lower than for the drug and shRNA/Lipofectamine.	
PLK1 siRNA	Liposome	Folate	PC3 and 22Rv1	BALB/c nude mice	Dual targeted liposomes with folate (for PSMA targeting) and a cleavable peptide that reveals a cell penetrating peptide in the presence of PSA. twofold greater KD of PLK1 mRNA by targeted NPs in 22Rv1 xenograft mouse model compared with the non-targeted control.	(Xiang *et al.*, 2013)
MiR-15a and miR-16-1	Atelocollagen	Aptamer 10–3.2	PC3 and LnCap cells	BALB/c nude mice	5.4 fold higher uptake efficiency with targeted formulation in LnCap cells miRNA complexed with targeted formulations four-fold lower IC50 value compared with untargeted forulation In a human PCa bone metastasis model, mean survival time for mice treated with miRNA/ATE was 38 days, while those treated with miRNA/ATE-APT had an average survival time of 57 days.	(Hao *et al.*, 2016)

Table 3

List of PSMA based therapeutics developed with focus on Immunotherapy and radiotherapy

Therapeutic payload	Delivery vector	Targeting ligand	*In vitro* model	*In vivo* model	Concluding remarks	References
Immunotherapy						
CD-40 Targeted adenovirus	CD-40 Targeted adenovirus	N/A	RM1 cells (PSMA+)	N/A	Only combination therapy of Ad5-huPSMA and Ad5-IFNγ resulted in delayed growth of RM1-PSMA tumours by CTL. Tumours that were PSMA- showed a weak inhibition of tumour growth.	(Williams *et al.*, 2012)
DCs treated with recombinant survivin and recombinant PSMA	N/A	N/A	N/A	Patient study	Response Evaluation Criteria In Solid Tumours was 72.7% for the DC group and 45.4% in the control group. The median overall survival of patients in the DC vaccine group improved by 11 months compared with the control group	(Xi *et al.*, 2015)
DCs	Adenovirus	N/A	RM1 cells (PSMA+)	N/A	DCs were transduced with Ad-tPSMA, Ad-m4-1BBL and Ad-tPSMA-m4-1BBL. Highest level of T-cell cytotoxicity in RM-1 cells (~60%) was seen in the group transduced with Ad-tPSMA-m4-1BBL.	(Youlin *et al.*, 2013)
T-cells	Lentivirus expressing CAR (J591)	N/A	MS1PSMA, H5VPSMA	NOD/SCID mice	*The CAR T-cells were shown to be capable of killing the PMSA+ cells while sparing the PSMA- lines *in vitro.* *In vivo;*full regression of PMSA+ MS1 tumours following dosing of CAR T-cells 24 days post tumour inoculation.	(Santoro *et al.*, 2014)
T-cells	Lentivirus expressing anti-human PSMA	N/A	LNCaP, PC-3	NOD/SCID, SCID	Specific CTL activity against PC-3 cells manipulated to express PSMA (PC-3-PIP), but not in wild type PC-3. *In vivo;* Detectable metastatic disease 21 post T-cell injection in control group, with no visible signs of PC-3 PIP cells after this point in the treated group.	(Zuccolotto *et al.*, 2014)
T-cells	Retrovirus expressing scFv of anti-human PSMA	N/A	PC-3 (PSMA+/−)	BALB/c nude mice	Specific cell lysis of PC-3PSMA, which was not observed in WT PC-3 cells. *In vivo*; In a PC-3 PSMA xenograft mouse model, 75% of mice treated with T-cells expressing anti-PSMA CARs were tumour free 27 days post inoculation.	(Ma *et al.*, 2014)
T-cells	Bispecific antibody	N/A	PC-3, LNCap	N/A	*Antibody constructs were able to elicit a T-cell response and resulted in subsequent	(Arndt *et al.*, 2014)

continues

Table 3 (Continued)

Therapeutic payload	Delivery vector	Targeting ligand	*In vitro* model	*In vivo* model	Concluding remarks	References
	targeting PSMA and PSCA				lysis of PC-3PSMA, PC-3PSCA, PC-3PSMA/PSCA when co-cultured with the constructs and inactivated t-cells.	
Genes encoding ttk and sFLT3L	Adenovirus	N/A	LNCaP, PC-3, DU-145, CWR22rv	N/A	Expression of "therapeutic" and viral replication genes and could only take place in cells expression PSMA and PSA. LNCaP/CWR22rv had higher levels of viral accumulation and cell death when compared with DU-145/PC-3.	(Kim *et al.*, 2013)
T-cells	Bispecific diabody targeting PSMA and CD3	N/A	LNCaP, C4–2, DU-145	N/A	Only in the presence of PMSA+ cells was there T-cell activation and expression of CD25 and CD69 in T-cells. C4–2 mice treated with T-cells + PSMA x CD3 diabody showed a lower tumour burden ($<200mm^3$) compared with the control groups ($>1500\ mm^3$).	(Fortmüller *et al.*, 2011)
T-cells	Electroporation of plasmid DNA vaccines encoding PSA and PSMA	N/A	N/A	BALB/C nude	Vaccines were delivered IM followed by electroporation. Plasmid vaccines induced a strong IFNγ and IL-2 response by CD4+ and CD8+ T-cells, with CD4+ also exhibiting a strong TNFα response.	(Ferraro *et al.*, 2011)
T-cells	DNA fusion vaccines w/PSMA/FrC of tetanus vaccine	N/A	TRAMP-C1	HHD mice	Fusion vaccines stimulated over 75% specific lysis of cells endogenously expressing PSMA. *In vivo;* Specific lysis of PSMA + cells was stimulated by the fusion vaccines in three quarters of mice tested.	(Vittes *et al.*, 2011)
Radiotherapy						
^{225}Ac	Liposomes	J591 antibody/ A10 Aptamer	LnCaP, Mat-Lu, HUVEC, BT474, and MDA-MB-231	N/A	J591-liposomes were more effective at binding to all cell lines compared with A10-liposomes. J591-liposomes loaded with ^{225}Ac was also the most cytotoxic liposomal construct tested.	(Bandekar *et al.*, 2014)
^{177}Lu	N/A	DKFZ-617 PSMA inhibitor	N/A	Human clinical study	10 patients with chemotherapy resistant and/or hormone refractory prostate cancer were treated with ^{177}Lu-DKFZ-617 PSMA. 70% of patients had a PSA decline, with 5 patients showing PSA decline >50%. ^{177}Lu-DKFZ-617 PSMA also exhibited a low early side effect profile.	(Ahmadzadehfar *et al.*, 2015)

continues

Table 3 (Continued)

Therapeutic payload	Delivery vector	Targeting ligand	*In vitro* model	*In vivo* model	Concluding remarks	References
^{177}Lu/^{68}Ga	–	DOTAGA-ffk (Sub-KuE)	LnCap cells	CD-1 nu/nu mice	This theranostic allows for combined diagnosis and therapy. The uptake of imaging and therapeutic agent was greatest in the tumour and kidneys (both PSMA expressing) 1 hour post injection in an LNCaP xenograft model (4.95% ID/g for ^{68}Ga-PSMA and 7.96% ID/g for ^{177}Lu-PSMA). Treatment of two patients with metastatic disease was shown to be effective with no side effects detected.	(Weineisen *et al.*, 2015)
^{177}Lu	N/A	DKFZ-11 PSMA inhibitor	N/A	Human clinical study	Following treatment, patient showed a radiological response and in addition, PSA levels fell from 38 to 4.6 ng/ml.	(Kratochwil *et al.*, 2015)
^{124}I/^{131}I	N/A	MIP-1095 PSMA inhibitor	N/A	Human clincal study	16 patients underwent 124I/^{131}I-MIP-1095 treatment. PSA levels fell by >50% in 60.7% of patients treated. 84.6% of patients that reported bone pain indicated either a complete or moderate pain relief. There were no significant haematological or renal toxicities reported.	(Zechmann *et al.*, 2014)
^{177}Lu	N/A	PSMA antibody J591	N/A	Human clinical study	47 hormone refractory patients were treated in a Phase II clinical trial with ^{177}Lu-J591. 10.6% AND 36.2% of patients received a ≥ 50% ≥ 30% decrease in PSMA levels respectively. There was a significantly longer survival (P = 0.03) in those patients receiving the maximum tolerated dose (21.8 vs 11.9 months). Patients with low PSMA expression were less likely to respond.	(Tagawa *et al.*, 2013), (Simone and Hahn, 2013)
^{177}Lu	N/A	DOTA-3/F11 (PSMA antibody)	C4–2 and DU145 cells	SCID mouse (C4–2 xenograft model)	Imaging agents showed T1/2 of >7 days *in vivo*. A single dose of ^{177}Lu-DOTA-3/F11 significantly slowed growth in C4–2 xenograft tumour model (<250 mm^3 tumour volume in treated group at day 20 versus >1500 mm^3 in the control group).	(Behe *et al.*, 2011)
^{125}I	N/A	DCIBzL PSMA inhibitor	PC3 PIP (PSMA+) and PC3 flu (PSMA-) and LnCap cells	Athymic nude mice	Uptake of ^{125}I-DCIBzL was significantly higher in PSMA PC-3 PIP (PSMA+) compared with PC-3 flu (PSMA-) cells. PC-3 PIP tumours showed significantly (p = 0.002) delayed growth when treated	(Kiess *et al.*, 2015)

continues

Table 3 (Continued)

Therapeutic payload	Delivery vector	Targeting ligand	*In vitro* model	*In vivo* model	Concluding remarks	References
					with ^{125}I-DCIBzL compared with PC-3 flu tumours.	
^{131}I	Adenovirus	hNIS	LnCap cells	BALB/c nude mice	A significantly higher uptake ($p = 0.0075$) of iodide was observed by xenograft tumours transfected with Ad.PSMApro-hNIS vs. Ad.CMV (2846.03 ± 188.29 c.p.p.mg −1 vs. 9.19 ± 1.00 c.p.p.mg −1 respectively).	(Gao *et al.*, 2014)
^{90}Y/^{177}Lu	N/A	PSMA antibody J591	N/A	Human clinical study	The single maximum tolerated dose (MTD) of ^{90}Y-J591 and ^{177}Lu-J5916. was 17.5 mCi/m2 and 70 mCi/m2. Several administrations over 4–6 months was well tolerated in patients where thrombocytopenia was manageable.	(Vallabhajosula *et al.*, 2005)
^{177}Lu	N/A	PSMA antibody J591	N/A	Human clinical study	35 patients received ^{177}Lu-J591. ^{177}Lu-J591 was able to target all skeletal and soft tissue metastasis (determined by MRI). *There was no immunogenic response to J591. Four patients had a > 50% decline in PSMA with 16 showing PSA stabilization for median 60 days.	(Bander *et al.*, 2005)
^{90}Y/^{131}I	N/A	PSMA antibody J591	LnCap cells	BALB/c nude mice	15–90% reduction in LNCaP xenograft tumour volume following a single dose of either ^{90}Y-J591 or ^{131}I-J591 was observed. *An increase in survival time two to threefold compared with untreated controls was also observed.	(Vallabhajosula *et al.*, 2005)

Table 4

List of PSMA based diagnostics developed for prostate cancer and neurological diseases

Imaging agent	Targeting ligand	*In vitro* model	*In vivo* model	Concluding remarks	References
Prostate cancer					
^{123}I	MIP-1072 and MIP-1095 (PSMA inhibitors)	N/A	Patient study	Both imaging agents were able to effectively detect lesions in bone, soft tissue and the prostate gland within 1 hour.	(Barrett *et al.*, 2013)
Iron oxide nanoparticles w/MRI	PSMA antibody J591	LnCap, DU145	N/A	Significantly higher uptake of targeted iron oxide nanoparticles in LNCap cells (PSMA+) (>1.4 mM of Fe) compared with DU145 (PSMA-) cells (<0.3 mM of Fe).	(Abdolahi *et al.*, 2013)
^{18}F	DCFBC (PSMA inhibitor)	N/A	Patient study	^{18}F- DCFBC identified 32 suspected metastatic lesions, with 21 identified by conventional imaging. All of the 11 additional sites identified were mostly in the bone.	(Cho *et al.*, 2012)
^{18}F	PSMA inhibitor 2-PMPA	N/A	BALB/c nude mice (LnCap xenograft model)	Introduction of ^{18}F did not affect binding affinity of 2-PMPA. Specific binding of imaging agent to LnCaP xenograft tumours was observed	(Graham *et al.*, 2012)
^{68}Ga	Urea-based PSMA inhibitor	LnCap and PC3 cells	BALB/c nude mice	The imaging agent was formed by the dimerization of the urea-based inhibitor coupled with ^{68}Ga. Dimer had better binding properties than the monomer (IC50 of 3.9 ± 1.8 nM for dimer vs. 12.1 ± 2.1 nM for monomer). There was a higher accumulation of agent in LnCaps (PSMA+) compared with PC3 (PSMA-) tumours; (8.22 ± 1.78% injected dose per gram 1 h post injection in LNCaP tumours versus 0.93 ± 0.53% in PC-3 tumours).	(Schäfer *et al.*, 2012)
IR800 and Cy5.5	Anionic PSMA ligand	PC3-PIP(PSMA+) and PC3-flu (PSMA-)	Athymic nude mice	High binding affinity in xenograft tumours derived from PC-3 cells transfected to express PSMA (PC3 PIP)	(Wang *et al.*, 2014)
^{111}In	Anti-PSMA nanobody JVZ-007	LNCaP, PC346C, VCaP, and MDA-PCa-2b, B16-PSMA	BALB/c nude mice	Effective labelling of LNCaP cells and PSMA expressing PDX models with no binding to PSMA-negative PDX models and kidneys.	(Chatalic *et al.*, 2015)
^{111}In	PSMA antibody J591	N/A	Patient study	In a 20 patient study, ^{111}In-J591 identified 74% of skeletal lesions, 53% of nodal lesions and 64% of other soft tissue lesions.	(Pandit-Taskar *et al.*, 2015b)
^{111}In/IRDye800CW	PSMA antibody D2B	LnCap, PC3, LS174T-PSMA	BALB/c nude mice	^{11}In-DTPA-D2B-IRDye800CW accumulated to a significantly greater level in LNCaP (PSMA+) tumours (45.8 ± 8.0% injected dose per gram	(Lütje *et al.*, 2014)

continues

Table 4 (Continued)

Imaging agent	Targeting ligand	*In vitro* model	*In vivo* model	Concluding remarks	References
				at 7 days post injection) compared with PC-3 tumours (6.6 ± 1.3% injected dose per gram at 7 days post injection).	
$^{125}I/^{111}In$	PSMA antibody capromab pendetide	LnCap and PC3 cells	BALB/c nude mice	Capromab binds to the intracellular domain of PSMA. There was less accumulation of ^{125}I in healthy organs compared with ^{111}In (1.6 fold lower in the colon and 2.3 fold in the bone).	(Tolmachev *et al.*, 2014)
^{18}F	Phosphoramidate PSMA inhibitor	LNCaP, CWR22Rv1, PC-3 cells	Athymic NCr-nu/nu mice	Increased uptake of imaging agent in PSMA + cells (2.2% in CWR22Rv1 and 12.1% in LNCaP cells) in comparison with PSMA – cells (0.08% in PC-3)	(Ganguly *et al.*, 2015)
^{18}F	DCFBC PSMA inhibitor	N/A	Patient study	Significantly lower uptake of ^{18}F-DCFBC by benign prostatic hypertrophy than primary tumours ($p = 0.004$). Able to detect higher grade (Gleason score 8 or 9) and larger tumours more effectively than MRI	(Rowe *et al.*, 2015)
^{18}F	2-PMPA PSMA inhibitor	22RV1, PC3, HEK293, V79 cells	BALB/c nude mice	High accumulation of imaging agent in LNCaP xenograft tumours. Safety studies indicated no off-target activity, effect on vital organ functions or dose-dependent adverse effects.	(Lesche *et al.*, 2014)
^{64}Cu	Binding domains of PSMA mAb 3/F11	LnCap, DU145, HEK293 cells	SCID mice	Two recombinant Anti-PSMA antibodies were conjugated to human IgG3 CH3 or Fc domain. There was accumulation of conjugated IgG3 CH3 (10.7 ± 2.0% injected dose per gram 48 h post injection) and IgG3 Fc (10.6 ± 1.4% injected dose per gram 48 h post injection) antibody fragments in PSMA + C4–2 tumours on xenograft model. However, uptake was less with the full length antibody (20.9 ± 2.2% injected dose per gram 48 h post injection for full length mAb).	(Wiehr *et al.*, 2014)
^{64}Cu	Urea-based PSMA inhibitor	PC3 cells	SCID mice	^{64}Cu-CB-TE2A displayed the most favourable kinetics and a high image contrast (29.50 ± 8.1% injected dose per gram 2 h post injection in PC-3 PIP tumours versus 0.66 ± 0.26% in PC-3 flu tumours).	(Banerjee *et al.*, 2014)
^{64}Cu	DUPA	PC3 and LnCap cells	SCID mice	Imaging agent was targeted to two biomarkers for prostate cancer, PSMA and gastrin-releasing peptide (GRPr). Maximum intensity was observed 18 h post injection in PSMA positive (LNCaP) and GRPr positive (PC-3) xenograft tumours.	(Bandari *et al.*, 2014)
^{68}Ga	Urea-based PSMA inhibitor	N/A	Patient study	Patient with biochemical relapse underwent lymph node dissection based on the results from imaging	(Schiavina *et al.*, 2015)

continues

Table 4 (Continued)

Imaging agent	Targeting ligand	*In vitro* model	*In vivo* model	Concluding remarks	References
				agent. Patient exhibited reduction in PSA following surgery.	
^{68}Ga	HBED-CC PSMA ligand	N/A	Patient study	^{68}Ga-PSMA-11 was able to detect lymph node metastasis in two-thirds of patients who would have been missed by conventional CT diagnosis	(Giesel *et al.*, 2015)
^{68}Ga/ ^{177}Lu-	DOTAGA-ffk (Sub-KuE)	LnCap cells	CD-1 nu/nu mice	In combination with radiotherapeutic ^{117}Lu, this theranostic exhibited a more favourable PK profile than DOTA conjugated, was rapidly internalized in PSMA + cells with minimal non-specific uptake.	(Weineisen *et al.*, 2014)
^{68}Ga	Urea-based PSMA inhibitor	N/A	Patient study	There was a significantly higher detection rate of positive lesions (59 vs 29) by ^{68}Ga-PSMA-HBED in patients with biochemical recurrence compared with ^{18}F-Fluoromethylcholine (FMC)	(Morigi *et al.*, 2015)
^{68}Ga	PSMA ligand HBED-CC	N/A	Patient study	In 70 patients with recurrent prostate cancer following primary treatment, 52/70 tested positive with ^{68}Ga; 30 patients had lesions in the pelvis, 8 had distant lesions and 14 had local plus systemic lesions.	(Ceci *et al.*, 2015)
^{68}Ga	PSMA ligand HBED-CC	N/A	Patient study	222/248 (89.5%) of patients with biochemical recurrence showed pathologic findings with ^{68}Ga-HBED-CC. Detection rated increased with increasing PSMA levels. ^{68}Ga-HBED-CC exclusively provided pathological findings in 81 (32.7%) patients.	(Eiber *et al.*, 2015)
^{68}Ga	PSMA ligand HBED-CC	N/A	Patient study	82.8% of patients had at least one prostate cancer lesion detected. Detection of tumours was positively associated with PSA level and androgen deprivation therapy.	(Afshar-Oromieh *et al.*, 2015)
^{68}Ga	PSMA ligand HBED-CC	LnCap, PC3, AR42J	BALB/c nude mice	Imaging agent was targeted to two biomarkers for prostate cancer, PSMA and gastrin-releasing peptide (GRPr). Reduction in intensity following blocking of the respective receptor (from 5.44 ± 1.54% to 1.06 ± 0.24% for LNCaP xenograft tumours).	(Eder *et al.*, 2014)
^{68}Ga & ^{18}F	PSMA ligands HBED-CC & DCFPyL	N/A	Patient study	^{18}F-DCFPyL was able to detect all lesions identified by ^{68}Ga-HBED-CC. In addition, ^{18}F-DCFPyL was able to detect three additional lesions. In PSMA positive lesions, the maximized standardized uptake value (SUVmax) was significantly higher with ^{18}F-DCFPyL than ^{68}Ga-HBED-CC (0.028)	(Dietlein *et al.*, 2015)

continues

Table 4 (Continued)

Imaging agent	Targeting ligand	*In vitro* model	*In vivo* model	Concluding remarks	References
^{68}Ga & ^{18}F	Urea-based PSMA inhibitor	N/A	Patient study	^{68}Ga-HBED-CC was able to detect all of the lesions detected by ^{18}F-fluoromethylcholine. In addition, ^{68}Ga-HBED-CC had a statistically higher detection rate ($p = 0.04$). The maximized standardized uptake value (SUVmax) was greater with ^{68}Ga-HBED-CC than^{18}F-fluoromethylcholine.	(Afshar-Oromieh *et al.*, 2014)
^{86}Y	ZJ43 PSMA inhibitor	PC3 cells	Papio Anubis (Baboon)	There was a greater uptake of targeted agents in PSMA positive (PC-3 PIP tumours) 5 h post injection (32.17 ± 7.99% injected dose per gram) compared with PC-3 flu tumours.	(Banerjee *et al.*, 2015)
^{89}Zr	PSMA antibody J591	N/A	Patient study	Compared with conventional imaging methods, ^{89}Zr-J591 detected 99 additional osseous sites. Accuracy of ^{89}Zr-J591 in prostate cancer detection was 95% for osseous sites and 60% for soft tissue lesions	(Pandit-Taskar *et al.*, 2015a)
^{99m}Tc	Diabody derived from J591	DU145 and LnCap cells	SCID mice	Significantly higher ($p < 0.001$) of accumulation of tracer in PSMA positive tumours (DU145-PSMA) (12.1 ± 1.7% injected dose per gram 8 h post injection) versus PSMA negative tumours (DU145) (6.3 ± 0.5% injected dose per gram 8 h post injection).	(Kampmeier *et al.*, 2014)
^{99m}Tc	Urea-based PSMA inhibitor	PC3 cells	NOD/SCID mice	[^{99m}Tc]L8 had the most favourable characteristics, with the lowest retention in normal tissues and higher accumulation in PSMA positive tumours compared with PSMA negative tumours (26.29 ± 7.45% injected dose per gram 2 h post injection in PC-3 PIP tumours versus 0.19 ± 0.08% in PC-3 flu tumours).	(Ray Banerjee *et al.*, 2013)
^{99m}Tc	MIP-1404 and MIP-1405 (PSMA inhibitors)	LnCap and PC3 cells	NCr-nu/nu mice	Both ^{99m}Tc-mip-1404 and 99mTc-mip-1405 were able to rapidly detect soft tissue prostate cancer lesions and more skeletal metastatic lesions compared with standard-of-care bone scanning	(Hillier *et al.*, 2013)
Indocyanine green (ICG)/ ^{125}I	Minibody (MB) against PSMA.	PC3 cells	Athymic nude mice	The minibody was conjugated to an activatable fluorophore, ICG. This would only fluoresce following PSMA binding. There was greater accumulation of tracer in PSMA positive cells (> 20% injected dose per gram 24 h post injection) than in PSMA negative tumours (< 5% injected dose per gram 24 h post injection).	(Watanabe *et al.*, 2014)
Biotin-streptavidin system	Anti-PSMA nanobody	LnCap, C4–2 and MKN45 cells	BALB/c nude mice	Arrival time, peak time, peak intensity and enhanced duration were all significantly different from blank	(Fan *et al.*, 2015)

continues

Table 4 (Continued)

Imaging agent	Targeting ligand	*In vitro* model	*In vivo* model	Concluding remarks	References
				nanobubbles in two PSMA + animal xenograft (LNCaP and C4–2)	
IRDye800CW	Urea-based PSMA inhibitor	U87-MG and PC3 cels	NOD/SCID mice	Imaging agent was targeted to two biomarkers for prostate cancer, PSMA and integrin-$\alpha v\beta_3$.	(Shallal *et al.*, 2014)
Iron oxide nanoparticles w/MRI	PSMA antibody J591	LNCaP, PC3, DU145, 22RV1, RWPE-1 and BPH-1 cells	NOD/SCID mice	Iron oxide nanoparticles were non-toxic to prostate cancer cells. Conjugation of J591 to iron oxide nanoparticles did not adversely affect its ability to bind PSMA. *In vivo* MRI of tumours was improved using PSMA targeted nanoparticles, but not with non-targeted nanoparticles.	(Tse *et al.*, 2015)
Iron oxide nanoparticles w/MRI	PSMA-targeting polypeptide (CQKHHNYLC, C1–C9 disulfide)	LnCap and Pc3 cells	BALB/c nude mice	The relative signal enhancement (RSE) in LNCaP cells treated with targeted iron oxide nanoparticles was significantly higher at 2, 6 and 12 h (19.9 ± 3.4, 34.3 ± 3.6, 30.9 ± 1.4 respectively) compared with PC-3 cells treated with targeted iron oxide nanoparticles (8.7 ± 2.2, 11.1 ± 3.1, 10.4 ± 2.6 respectively).	(Zhu *et al.*, 2015)
^{18}F	PSMA ligand DCFPyL	PC3 and 22RV1 cells	NOD/SCID mice	Greater accumulation of tracer in PSMA positive tumours (PC-3 PIP) (39.4 ± 5.4% injected dose per gram 1 hour post injection) versus PSMA negative tumours (PC-3) (0.11 ± 0.02% injected dose per gram)	(Chen *et al.*, 2011)
Iron platinum nanoparticles w/MRI	PSMA antibody J591	C4–2 and PC3 cells	N/A	Iron platinum nanoparticles were encapsulated by PEGylated phospholipids in order to create stealth nanoparticles that were targeted to PSMA positive cells with J591.	(Taylor *et al.*, 2011)
^{89}Zr	PSMA antibody 7E11	LnCap and PC3 cells	SCID mice	There was high levels of target-specific uptake of ^{89}Zr-7E11 in LNCaP cells (20.35 ± 7.50% injected dose per gram 34 h post injection)	(Ruggiero *et al.*, 2011)
CdSe/CdTe	Apatamer A9	LnCap and PC3 cells	N/A	Aptamer-nanocrystal conjugates showed specific binding of live and fixed cells, and were also able to target PSMA positive cells that were dispersed in a collagen gel matrix.	(Chu *et al.*, 2006)
Cy5	Apatamer A10	CPA, LnCap and PC3 cells	BALB/C nude mice	Aptamer-targeted nanoparticles were found to only target PSMA positive LNCaP and canine prostate adenocarcinoma cells, but not PC-3 cells.	(Tong *et al.*, 2010)
Fluorescent quantum dot (QD)	Apatamer A10	LnCap and PC3 cells	N/A	There was specific binding of Aptamer-targeted QDs to LNCaP cells with no uptake into PC-3 cells. When the particles were loaded with Docetaxel, there was a significant reduction of cell viability in LNCaP	(Bagalkot *et al.*, 2007)

continues

Table 4 (Continued)

Imaging agent	Targeting ligand	*In vitro* model	*In vivo* model	Concluding remarks	References
				cells compared with PC-3 cells (approximately 50% cell viability versus 75% respectively).	
Neurological disorders					
^{68}Ga	Urea-based PSMA inhibitor	N/A	Human brain tissue	Increased accumulation of ^{68}Ga-HBED-CC-PSMA was observed in tumour areas of the brain, with no uptake in unaffected brain regions IHC confirmed increased PSMA expression in tumour vasculature.	(Schwenck *et al.*, 2015)
^{125}I	PSMA ligand DCIT	N/A	Rodent brain tissue	Autoradiography of rodent brain sections was used to detect GCPII. Imaging of brain with ^{125}I-DCIT was reduced in knockout mice in a gene-dose-dependent manner, thus indicating its binding specificity. The goal was to develop an imaging agent that quantitatively determines GCPII levels *in vivo*	(Guilarte *et al.*, 2005)
^{125}I	PSMA ligand DCIT	N/A	Human brain tissue	Autoradiography of human brain sections was used to detect GCPII. Patients with schizophrenia had significantly lower levels of GCPII in the prefrontal cortex and entorhinal cortex compared with age matched controls. Highlights benefit of GCPII imaging agent in the diagnosis of neurological disease.	(Guilarte *et al.*, 2008)
^{11}C	Urea-based PSMA inhibitor	N/A	CD-1 mice	Brain uptake of ^{11}C-MCG was low, highlighting that the agent may be inappropriate for monitoring brain GCP II activity. This was thought to be due to the hydrophilic nature of the agent (logP = −0.235)	(Pomper *et al.*, 2002)

Gene therapy

In recent years, advances in the field of next generation sequencing has brought the fields of gene and RNA interference (RNAi) therapy closer to the clinic. While gene therapy involves the replacement of a defective or deleted gene in a cell or tissue, RNAi therapy involves the silencing of a target gene (i.e. disease causing gene) in a sequence-specific manner, using double stranded RNA (dsRNA) (Grimm and Kay, 2007; Guo *et al.,* 2013a). Provided that the dsRNA is appropriately designed, RNAi has the potential to silence (theoretically) any gene within the genome (Jackson and Linsley, 2010). In recent years, the PSMA/GCPII has been used to successfully target siRNA, shRNA, microRNA or therapeutic genes to PSMA/GCPII positive cells (Table 2).

A recent study incorporated a PSA responsive element and a PSMA/GCPII targeted component into a liposome for the treatment of PCa. DSPE-PEG_{5000}-folate was used to target the liposome to the PSMA/GCPII receptor in a 22rv1 xenograft model of PCa. This multifunctional liposome showed preferential binding to cells that secreted PSA and expressed PSMA/GCPII. There was a significant reduction in tumour burden and target mRNA (Plk1) in a xenograft tumour model (Xiang *et al.,* 2013). Plk1 is a key regulator of cell mitosis, and its inhibition has been shown to induce apoptosis in rapidly dividing tumour cells (Strebhardt and Ullrich, 2006; Dassie *et al.,* 2009).

In two-thirds of metastatic breast and PCa patients, there is some spread of the disease to the bone (www.cancer.org). Bone metastases can be painful and debilitating for the patient, and generally result in significant morbidity, with most therapeutic interventions offering only modest benefits (Takeshita *et al.,* 2010). A second generation RNA aptamer (A10–3.2) targeting PSMA/GCPII has been used to deliver microRNA (miR-15a and miR-16-1) to bone metastases using atellocollagen as a delivery vector (Hao *et al.,* 2016). The resulting construct showed significantly higher levels of uptake in PSMA positive LNCaP cells *in vitro* compared with PSMA/GCPII negative PC3 cells. The construct containing the PSMA/GCPII aptamer also significantly increased the survival times in a mouse model of human PCa bone metastasis.

One approach currently under investigation for PSMA/GCPII-mediated gene therapy is suicide gene therapy. This is where a gene encoding an enzyme that converts a non-toxic prodrug into a highly toxic compound is delivered into tumour cells (Dachs *et al.,* 2005). In a recent study, the HSV-thymidine kinase (TK) and connexin43 gene was delivered to PSMA/GCPII positive LNCaP cells using a PAMAM dendrimer delivery vector with folate as a targeting ligand for PSMA/GCPII (Chen *et al.,* 2013). The expression of TK and connexin43 was driven by the PSMA/GCPII promoter, thus they could only be expressed in PSMA/GCPII positive cells, with no detectable gene expression in PSMA/GCPII negative PC3 cells. This example of the double-targeting of PSMA/GCPII highlights the therapeutic advantages of targeting this receptor.

Immunotherapy

The role of the immune system to seek out and destroy cancer tumour cells is well documented (Apetoh *et al.,* 2015). The ability of the immune system to control the growth of tumours can be demonstrated in patients with an immunodeficiency such as HIV, in whom the cancer burden is far greater than in the uninfected population (Robbins *et al.,* 2015). Several decades of research into immunotherapy have recently started to show returns with several immunotherapies in clinical trials and approved for use in recent years (Rowdo *et al.,* 2015). Several highly effective immunotherapies at both the preclinical and clinical stage targeting PSMA/GCPII are summarized in Table 3.

Dendritic cells (DCs) are classed as effective antigen presenting cells, initiating and directing a T-cell response, thus making them ideal candidates as the powerhouses for a cancer vaccine (Palucka and Banchereau, 2012). DCs function by eliciting the activation of T-cells. This activation occurs when DCs present antigens to naïve CD8+ cells (via MHCI) and CD4+ cells (via MHCII). This results in the maturation of T-cells and can induce a cytotoxic T-lymphocyte (CTL) response against the cancer cell carrying the offending antigen. Several studies have highlighted the potential of DCs that have been modified *ex vivo* to elicit a CTL response in patients (Fuessel *et al.,* 2006; Waeckerle-Men *et al.,* 2006; Fishman, 2009).

In a recent study, DCs were primed with recombinant survivin and recombinant PSMA (Xi *et al.,* 2015). These DCs were then used in a clinical study of 21 patients with castration-resistant PCa, with docetaxel and prednisone used as a control. Objective response rate by Response Evaluation in Solid Tumours was 8/11 in patients who received DC therapy, with an increased survival time and 2 patients showing partial remission. Another study using DC based therapy involved the transfection of DCs with adenovirus expressing human PSMA (huPSMA) and IFNγ (Williams *et al.,* 2012). The results of this study showed a delayed growth of RM1-PSMA/GCPII tumours and a significant increase in cytotoxic T-cell activity in mice treated with a combination of Ad5-huPSMA and Ad5- IFNγ, with weak tumour inhibition observed in PSMA/GCPII negative tumours.

Apart from DCs, there has been a move to develop T-cells bearing a chimeric antigen receptor (CAR) against PSMA/GCPII to elicit CTL activity against PSMA/GCPII positive tumour cells (Ma *et al.,* 2014; Santoro *et al.,* 2014; Zuccolotto *et al.,* 2014). CAR technology has already shown promising efficacy in acute and chronic lymphoid leukaemia (Porter *et al.,* 2011; Grupp *et al.,* 2013). In the case of PSMA/GCPII, these T-cells are generated by the transduction of naïve T-cells using a virus that encodes some form of anti-PSMA/GCPII antibody along with co-stimulatory signalling domains such as CD-28 and 4-1BB which drives T-cell maturation (Santoro *et al.,* 2014). A NOD/SCID mouse model inoculated with modified PC3 cells to express PSMA/GCPII (PC3-PIP) was treated using a T-body (genetically engineered T-cell carrying a chimeric receptor [Eshhar, 2008)] directed against PSMA/GCPII. These T-cells had previously shown specific lysis against PSMA/GCPII positive cells only and, *in vivo,* they were able to inhibit the formation of metastasis, with no visible signs of any PC3-PIP cells present, 21 days after the injection of the T-cells (Zuccolotto *et al.,* 2014).

Immunotherapy (while still in the early stages), has shown great therapeutic potential, and as it exploits the host's own immune system to fight the disease it offers long term protection against the relapse of cancer.

Radiotherapy

Radiation therapy (also called ionizing radiation) has been used to treat cancer for over 100 years since the discovery of X-rays in 1895 (Thariat *et al.*, 2013). Today, nearly half of all cancer patients routinely receive radiotherapy either alone, or else in combination with other treatments such as surgery or chemotherapy (Delaney *et al.*, 2006). In PCa, approximately 25% of patients with localized disease will undergo some form of radiotherapy (Cooperberg *et al.*, 2010). Radiation deposits high levels of energy in tissues and cells as it passes through them, damaging genetic material in the process. In doing so, the aim is that the cancer cells lose their ability to grow and divide (Jackson and Bartek, 2009; Baskar *et al.*, 2012).

The most common radionuclides used in radiotherapy are ^{90}Y, ^{131}I and ^{177}Lu. Due to the differing physical properties of the different radionuclides, each one may be suited to an optimal tumour size and type (Bouchelouche *et al.*, 2010). For example, ^{177}Lu is more suited for the treatment of smaller tumours (1–3 mm) while ^{90}Y is suited to treat larger tumours (28–42 mm) (O'donoghue *et al.*, 1995). In recent years, traditional radiotherapy has reduced unwanted side effects, allowing an increase in dosage. The addition of a targeting ligand, such as a monoclonal antibody or aptamer, to a radionuclide allows for the targeting of a cancer-associated cell-surface antigen. This is known as radioimmunotherapy (RIT) and, while traditionally RIT is more effective in more radiosensitive tumours, such as leukaemias and lymphomas, there is now a move towards using RIT to treat the more radioresistant solid tumours (Larson *et al.*, 2015).

The PSMA/GCPII has been a desirable target for RIT for many years, with a summary of studies involving the delivery of RIT using PSMA/GCPII given in Table 3. The first anti-PSMA/GCPII antibody that was used for RIT and imaging was capromab (7E11/CYT-356) (Kahn *et al.*, 1998a; Kahn *et al.*, 1998b). The initial results from this therapy were disappointing, as capromab binds to the intracellular domain of PSMA/GCPII, and so will only bind to dying or permeable cells (Bouchelouche *et al.*, 2010). In addition, in a phase II clinical trial with ^{90}Y-capromab, there was significant toxicity (myelosuppression), and another study was prematurely terminated due to a lack of efficacy (no decline in PSA level or radiological response) (Deb *et al.*, 1996; Kahn *et al.*, 1999).

In response to this, second generation antibodies have been developed that target the extracellular domain of PSMA/GCPII. Such antibodies that have been widely researched in recent years for PCa RIT include 3F/11 (Behe *et al.*, 2011) and J591 (Vallabhajosula *et al.*, 2004; Bander *et al.*, 2005; Vallabhajosula *et al.*, 2005; Simone and Hahn, 2013; Tagawa *et al.*, 2013; Bandekar *et al.*, 2014), which unlike its predecessors can bind living cells (Smith-Jones *et al.*, 2000). In a phase II clinical trial, a single infusion of ^{177}Lu-J591 was administered to two cohorts of patients ($n = 47$) with metastatic PCa. Of the 47 patients in the trial, 10.6% had a greater than 50% decrease in their PSA levels, 36.2% had greater than 30% reduction and 59.6% showed at least some level of PSA decline. The therapy was well tolerated with all patients showing reversible haematological toxicity and there was also a significant increase in survival time (21.8 vs. 11.9 months) (Simone and Hahn, 2013; Tagawa *et al.*, 2013). The outcome of this trial indicates the benefits that PSMA/GCPII-mediated RIT can offer patients with metastatic disease.

Over the years, different PSMA/GCPII inhibitors have also been used to target radionuclides to PCa cells. As already mentioned, there are many different classes of inhibitors that have been developed to target the PSMA/GCPII. In terms of radionuclide delivery, these mainly constitute the urea-based inhibitors (Zechmann *et al.*, 2014; Ahmadzadehfar *et al.*, 2015; Kiess *et al.*, 2015; Kratochwil *et al.*, 2015; Weineisen *et al.*, 2015). In a recent clinical trial, 10 patients with hormone-refractory and/or chemotherapy-resistant PCa with confirmed metastasis were treated with ^{177}Lu, which was conjugated to the urea-based DKFZ-617 PSMA/GCPII inhibitor. Eight weeks following treatment, 70% of the patients experienced some level of PSA decline, with five showing a greater than 50% decline. Sixty per cent of patients showed no haematotoxicity following treatment and none exhibited nephrotoxicity. This study shows the therapeutic potential of a single dose of ^{177}Lu-DKFZ-617 in metastatic PCa patients that have no other therapeutic options (Ahmadzadehfar *et al.*, 2015).

Another recent study involved the transfection of PCa cells with an adenovirus containing the gene for the human sodium iodide symporter (hNIS) (Gao *et al.*, 2014). The expression of this hNIS gene was dependent on the expression of PSMA/GCPII in the target cell. Under normal conditions, hNIS is utilized by the thyroid gland to allow for far higher levels of iodide to accumulate in the gland compared with plasma (De la Vieja *et al.*, 2000). This usually allows for effective therapy of thyroid cancer with radioiodine (even in advanced cases) (Mazzaferri and Kloos, 1996). In an LNCaP Xenograft mouse model, there were significantly greater levels of iodide in animals treated with AD.PSMApro-hNIS compared with the control, and as such, these tumours had the lowest volume. This shows the potential benefits offerred by a combination of gene and radiotherapy in the treatment of advanced PCa.

PSMA/GCPII as a diagnostic tool

PSMA/GCPII-targeting ligands including PSMA/GCPII antibodies, aptamers and low molecular weight molecules and inhibitors have been used to target effective imaging agents including ^{64}Cu, ^{18}F, ^{68}Ga, ^{111}In, ^{99m}Tc and others such as iron oxide nanoparticles and IRDye 800. These studies are summarized in Table 4. A significant reduction in mortality from PCa in recent years has been attributed to earlier detection, but this has come at a price, with a number of (in some cases) unnecessary treatments being administered, which can have a negative impact on the patient's quality of life (Resnick *et al.*, 2013). In recent years, there has been a call to move away from the use of PSA as a diagnostic for PCa as it has been responsible for over-diagnosis of patients who may only require active surveillance (Etzioni *et al.*, 2002; Donovan, 2012). In this regard, the need for new biomarkers for effective diagnosis of lethal forms of PCa only is an unmet clinical need.

The J591 monoclonal antibody has been successfully used to image PCa metastasis in several studies. In a 20 patient study, ^{111}In-J591 was used to successfully identify 74% of

skeletal lesions, 53% of nodal lesions and 64% of other soft tissue lesions (Pandit-Taskar *et al.,* 2015b), while in a 50 patient study of metastatic PCa, ^{89}Zr-J591 detected 99 additional osseous sites compared with conventional imaging modalities (Pandit-Taskar *et al.,* 2015a), and ^{99m}Tc-J591 showed a significantly higher accumulation in PSMA/GCPII positive tumours (DU-145-PSMA) (12.1 ± 1.7% injected dose per gram 8 h post injection) compared with that in PSMA/GCPII negative tumours (DU-145) (6.3 ± 0.5% injected dose per gram 8 h post injection) (Kampmeier *et al.,* 2014). Despite the advantages offered by mAb imaging, they are usually associated with a delay in target recognition and background clearance in a suitable timeframe for diagnostic imaging (Osborne *et al.,* 2013).

Low molecular weight agents may provide more suitable pharmacokinetics for imaging (Bouchelouche *et al.,* 2010). Recently, a PSMA/GCPII phosphoramidate-based inhibitor was conjugated to ^{18}F for imaging. Uptake of the imaging agent in PSMA/GCPII positive LNCaP cells (12.1%) was much higher than in PSMA/GCPII negative PC3 cells (0.08%) (Ganguly *et al.,* 2015). Low molecular weight PSMA/GCPII inhibitors, MIP-1404 and MIP-1405 were linked to ^{99m}Tc, which were capable of detecting more skeletal metastatic lesions when compared with conventional imaging (Hillier *et al.,* 2013). A urea-based PSMA/GCPII inhibitor conjugated to ^{68}Ga was recently used to image 248 patients with biochemical recurrence following radical prostatectomy (Eiber *et al.,* 2015). 222/248 (89.5%) of patients with biochemical recurrence showed pathological findings with ^{68}Ga-HBED-CC. The rate of detection increased with higher PSA levels and ^{68}Ga-HBED-CC highlighted an additional 81 pathological findings, not identified by conventional imaging.

Another alternative to using mAb imaging is the use of aptamers. Recently, fluorescent quantum dots (QD) were conjugated to the aptamer A10. These imaging agents showed specific binding to PSMA/GCPII positive LNCaP cells, with no uptake in PC-3 cells. Also, when docetaxel was loaded onto the QDs, there was a significant reduction of cell viability in LNCaP cells compared with PC-3 cells (approximately 50% and 25% reductions respectively) (Bagalkot *et al.,* 2007).

In addition to conventional radionuclide imaging, other modalities targeting PSMA/GCPII have been developed in recent years. PSMA/GCPII-targeted iron oxide nanoparticles combined with magnetic resonance imaging (MRI) have shown encouraging results. J591-iron oxide nanoparticles show significantly higher uptake of targeted iron oxide nanoparticles in PSMA/GCPII positive (LNCap) cells compared with PSMA/GCPII negative (DU145) cells, and *in vivo* MRI of tumours was improved using PSMA/GCPII targeted nanoparticles, but not with non-targeted nanoparticles (Abdolahi *et al.,* 2013; Tse *et al.,* 2015).

While showing enormous potential and efficacy in the case of PCa, evidence of exploiting PSMA/GCPII as a diagnostic tool for neurological disorders has been scarce with relatively few studies published in the area (Table 4). Autoradiography of human brain sections using ^{125}I-DCIT showed that patients with schizophrenia had a significantly lower level of GCPII expression in the prefrontal cortex and entorhinal cortex, compared with age matched controls (Guilarte *et al.,* 2008). This study highlights the benefit of GCPII imaging agents in the diagnosis of neurological disease. However, there are major shortcomings for real time *in vivo* imaging of GCPII expression in the brain. A urea-based PSMA/GCPII inhibitor conjugated to ^{11}C showed low brain uptake in primates. This was thought to be due to the hydrophilic nature of the agent decreasing its ability to cross the BBB (Pomper *et al.,* 2002). A study was carried out in 2015 where GCPII was successfully imaged in the neovasculature of glioblastoma in a human patient using ^{68}Ga and a urea-based inhibitor of PSMA/GCPII (Schwenck *et al.,* 2015). Currently, work is ongoing to modify inhibitors to make them more applicable for use in neurological disease (Wang *et al.,* 2010; Feng *et al.,* 2011; Majer *et al.,* 2016).

Conclusions

PSMA/GCPII is a transmembrane protein that is highly expressed in PCa tissues and in the neovasculature of other tumour types, as well as in the brain. PSMA/GCPII plays a key role as a biomarker capable of diagnosing and staging PCa, and thus, many therapeutic and diagnostic agents have been developed that take advantage of recognizing this protein (Akhtar *et al.,* 2011; Demirkol *et al.,* 2015). Due to the multifunctional nature of PSMA/GCPII, its role in different areas of the body can be exploited for various biomedical applications including the treatment of PCa and neurodegenerative disease. Its function as a cell-surface ligand-binding receptor has been utilized to develop therapies that exploit the advantage of receptor-mediated endocytosis of therapeutic agents. This protein also acts as a hydrolysing enzyme to enhance the absorption of substrates from tissue to the blood stream (e.g. folate absorption from small intestine to blood stream) (Chang *et al.,* 2004). PSMA/GCPII has a similar hydrolysing activity in the brain, where it hydrolyzes NAAG into glutamates, which in certain cases causes glutamate toxicity. Glutamate toxicity triggers a set of signalling molecules that lead to degenerative processes causing cell death. Such degenerative effects are characteristic of diseases like dementia, ALS, schizophrenia, multiple sclerosis (Rahn *et al.,* 2012).

Historically, CNS therapies developed tend to be NAAG-catabolism inhibitors that block the NAAG hydrolysing capacity of the PSMA/GCPII protein. Although such therapies have shown success in preclinical studies, their translation to clinical setting has been a challenge due to the poor passage of the PSMA/GCPII inhibitors through the BBB (Bařinka *et al.,* 2012). Most of the inhibitor molecules developed are hydrophilic in nature and have high molecular weight, which acts as a limitation to delivery and, although certain approaches have been pursued to develop more hydrophobic drugs, very little success has been achieved in this area (Kozikowski *et al.,* 2004).

From an evolutionary point of view, it is interesting to consider what conditions drove the development of a receptor with two very different functions depending on where it is expressed, an area that has received very little or no attention, so far. This multifunctionality of PSMA/GCPII provides opportunities for two different therapeutic approaches: (i) as a receptor ligand and (ii) as a hydrolysing enzyme. For targeted therapeutic purposes, it can be used as a facilitator to deliver drugs or therapies to PCa cells. A number of studies describe the use of PSMA/GCPII specific ligands, such as

antibodies, aptamers, folate molecules attached or conjugated to therapeutic molecules (drugs, genes and radiolabelled-diagnostic molecules) or modified on the surface of nanoparticles for receptor-specific delivery. This strategy has been heavily exploited for PCa, as discussed above. While this has not been exploited for the treatment of neurological disorders and brain cancers, at present, two clinical trials are underway (results not yet disclosed) that use antibody-drug conjugates targeting PSMA/GCPII to treat patients with the highly invasive glioblastoma (NCT02067156, NCT01856933). It is hoped that the results of these trials will highlight the usefulness of targeting the PSMA/GCPII in brain malignancies.

Another potential approach for treating neurological disorders would be to knock-down (KD) the PSMA/GCPII transmembrane protein in the brain regions, instead of blocking it with inhibitors. Such KD of the PSMA/GCPII protein would have clinical effects, similar to those of the inhibitor drugs. The RNAi-mediated approach to KD of certain receptors and transporters in the brain has previously been successfully applied to other neurological conditions such as depression, wherein the siRNA-mediated KD of a 5-HT transporter lead to increased 5-HT signalling, nullifying the effect of corticosterone-induced stress in animals and resulting in improved cognitive and behavioural functions (Thakker *et al.,* 2005; Wu *et al.,* 2016). This approach is emerging as a new model of therapy instead of drugs and inhibitors that cannot cross the BBB. The evolving strategies in developing non-viral nanoparticles or therapeutic conjugate molecules for specific targeting and delivery of RNAi molecules, drugs or radio-ligands will further enhance the understanding of novel therapies and diagnoses developed for PSMA/GCPII. However, for this approach to be feasible, the dual delivery barrier of transport across the BBB and cell-specific uptake must be addressed. In order to tackle these delivery challenges, a recent study employed a bispecific antibody which simultaneously targeted the Tfr (allowing for crossing of the BBB) and BACE1. This approach resulted in reduced production of amyloid-β plaques in the brain of monkeys, thereby offering a promising therapeutic in the treatment of Alzheimer's disease (Yu *et al.,* 2014). If such a targeting mechanism was incorporated into a nanoparticle loaded with siRNA targeting PSMA/GCPII, this would offer a promising therapeutic strategy for various neurological disorders.

In conclusion, while the PSMA/GCPII offers many exciting opportunities for developing diagnostics and therapeutics in the PCa field, the potential for using the PSMA/GCPII for neurological disorders has been under-explored, due mainly to the complex issues surrounding delivery of drugs across the BBB. However, if these were resolved, targeting the PSMA/GCPII would be a very promising target for neurological disorders.

Acknowledgements

This work is supported by the Irish Cancer Society via a Research Scholarship to JCE (CRS12EVA) and a Project Grant to COD (PCI11ODR). The authors would also like to acknowledge the Irish Research Council for research funding (GOIPD/2014/151) and a FRSQ postdoctoral fellowship to MM.

Conflict of interest

The authors declare no conflicts of interest.

References

Abdel-Hadi M, Ismail Y, Younis L (2014). Prostate-specific membrane antigen (PSMA) immunoexpression in the neovasculature of colorectal carcinoma in Egyptian patients. Pathol Res Pract 210: 759–763.

Abdolahi M, Shahbazi-Gahrouei D, Laurent S, Sermeus C, Firozian F, Allen BJ *et al.* (2013). Synthesis and in vitro evaluation of MR molecular imaging probes using J591 mAb-conjugated SPIONs for specific detection of prostate cancer. Contrast Media Mol Imaging 8: 175–184.

Afshar-Oromieh A, Avtzi E, Giesel FL, Holland-Letz T, Linhart HG, Eder M *et al.* (2015). The diagnostic value of PET/CT imaging with the 68Ga-labelled PSMA ligand HBED-CC in the diagnosis of recurrent prostate cancer. Eur J Nucl Med Mol Imaging 42: 197–209.

Afshar-Oromieh A, Zechmann CM, Malcher A, Eder M, Eisenhut M, Linhart HG *et al.* (2014). Comparison of PET imaging with a 68Ga-labelled PSMA ligand and 18F-choline-based PET/CT for the diagnosis of recurrent prostate cancer. Eur J Nucl Med Mol Imaging 41: 11–20.

Ahmadzadehfar H, Rahbar K, Kürpig S, Bögemann M, Claesener M, Eppard E *et al.* (2015). Early side effects and first results of radioligand therapy with 177Lu-DKFZ-617 PSMA of castrate-resistant metastatic prostate cancer: a two-centre study. EJNMMI Res 5: 1–8.

Akhtar NH, Pail O, Saran A, Tyrell L, Tagawa ST (2011). Prostate-specific membrane antigen-based therapeutics. Adv Urol 2012. doi:10.1155/2012/973820.

Alexander SP, Davenport AP, Kelly E, Marrion N, Peters JA, Benson HE *et al.* (2015a). The Concise Guide to PHARMACOLOGY 2015/16: Enzymes. Br J Pharmacol 172: 6024–6109.

Alexander SP, Davenport AP, Kelly E, Marrion N, Peters JA, Benson HE *et al.* (2015b). The Concise Guide to PHARMACOLOGY 2015/16: Catalytic receptors. Br J Pharmacol 172: 5979–6023.

Alexander SP, Davenport AP, Kelly E, Marrion N, Peters JA, Benson HE *et al.* (2015c). The Concise Guide to PHARMACOLOGY 2015/16: G protein-coupled receptors. Br J Pharmacol 172: 5729–5743.

Alexander SP, Davenport AP, Kelly E, Marrion N, Peters JA, Benson HE *et al.* (2015d). The Concise Guide to PHARMACOLOGY 2015/16: Transporters. Br J Pharmacol 172: 6110–6202.

Alexander SP, Davenport AP, Kelly E, Marrion N, Peters JA, Benson HE *et al.* (2015e). The Concise Guide to PHARMACOLOGY 2015/16: Nuclear hormone receptors. Br J Pharmacol 172: 5956–5978.

Anilkumar G, Barwe SP, Christiansen JJ, Rajasekaran SA, Kohn DB, Rajasekaran AK (2006). Association of prostate-specific membrane antigen with caveolin-1 and its caveolae-dependent internalization in microvascular endothelial cells: implications for targeting to tumor vasculature. Microvasc Res 72: 54–61.

Anilkumar G, Rajasekaran SA, Wang S, Hankinson O, Bander NH, Rajasekaran AK (2003). Prostate-specific membrane antigen association with filamin A modulates its internalization and NAALADase activity. Cancer Res 63: 2645–2648.

Apetoh L, Ladoire S, Coukos G, Ghiringhelli F (2015). Combining immunotherapy and anticancer agents: the right path to achieve cancer cure? Ann Oncol. doi:10.1093/annonc/mdv209.

Arndt C, Feldmann A, Koristka S, Cartellieri M, Dimmel M, Ehninger A *et al.* (2014). Simultaneous targeting of prostate stem cell antigen and prostate-specific membrane antigen improves the killing of prostate cancer cells using a novel modular T cell-retargeting system. Prostate 74: 1335–1346.

Baek SE, Lee KH, Park YS, Oh D-K, Oh S, Kim K-S *et al.* (2014). RNA aptamer-conjugated liposome as an efficient anticancer drug delivery vehicle targeting cancer cells in vivo. J Control Release 196: 234–242.

Bagalkot V, Zhang L, Levy-Nissenbaum E, Jon S, Kantoff PW, Langer R *et al.* (2007). Quantum dot-aptamer conjugates for synchronous cancer imaging, therapy, and sensing of drug delivery based on bi-fluorescence resonance energy transfer. Nano Lett 7: 3065–3070.

Baiz D, Hassan S, Choi YA, Flores A, Karpova Y, Yancey D *et al.* (2013). Combination of the PI3K inhibitor ZSTK474 with a PSMA-targeted immunotoxin accelerates apoptosis and regression of prostate cancer. Neoplasia 15: 1172–IN1132.

Bandari RP, Jiang Z, Reynolds TS, Bernskoetter NE, Szczodroski AF, Bassuner KJ *et al.* (2014). Synthesis and biological evaluation of copper-64 radiolabeled [DUPA-6-Ahx-(NODAGA)-5-Ava-BBN (7-14) NH 2], a novel bivalent targeting vector having affinity for two distinct biomarkers (GRPr/PSMA) of prostate cancer. Nucl Med Biol 41: 355–363.

Bandekar A, Zhu C, Jindal R, Bruchertseifer F, Morgenstern A, Sofou S (2014). Anti–prostate-specific membrane antigen liposomes loaded with 225Ac for potential targeted antivascular α-particle therapy of cancer. J Nucl Med 55: 107–114.

Bander NH, Milowsky MI, Nanus DM, Kostakoglu L, Vallabhajosula S, Goldsmith SJ (2005). Phase I trial of 177lutetium-labeled J591, a monoclonal antibody to prostate-specific membrane antigen, in patients with androgen-independent prostate cancer. J Clin Oncol 23: 4591–4601.

Banerjee SR, Foss CA, Pullambhatla M, Wang Y, Srinivasan S, Hobbs RF *et al.* (2015). Preclinical evaluation of 86Y-labeled inhibitors of prostate-specific membrane antigen for dosimetry estimates. J Nucl Med 56: 628–634.

Banerjee SR, Pullambhatla M, Foss CA, Nimmagadda S, Ferdani R, Anderson CJ *et al.* (2014). 64Cu-labeled inhibitors of prostate-specific membrane antigen for PET imaging of prostate cancer. J Med Chem 57: 2657–2669.

Bařinka C, Rojas C, Slusher B, Pomper M (2012). Glutamate carboxypeptidase II in diagnosis and treatment of neurologic disorders and prostate cancer. Curr Med Chem 19: 856.

Barinka C, Šácha P, Sklenář J, Man P, Bezouška K, Slusher BS *et al.* (2004). Identification of the N-glycosylation sites on glutamate carboxypeptidase II necessary for proteolytic activity. Protein Sci 13: 1627–1635.

Barrett JA, Coleman RE, Goldsmith SJ, Vallabhajosula S, Petry NA, Cho S *et al.* (2013). First-in-man evaluation of 2 high-affinity PSMA-avid small molecules for imaging prostate cancer. J Nucl Med 54: 380–387.

Baskar R, Lee KA, Yeo R, Yeoh K-W (2012). Cancer and radiation therapy: current advances and future directions. Int J Med Sci 9: 193.

Becker I, Lodder J, Gieselmann V, Eckhardt M (2010). Molecular characterization of N-acetylaspartylglutamate synthetase. J Biol Chem 285: 29156–29164.

Behe M, Alt K, Deininger F, Buehler P, Wetterauer U, Weber WA *et al.* (2011). In vivo testing of 177Lu-labelled anti-PSMA antibody as a new radioimmunotherapeutic agent against prostate cancer. In Vivo 25: 55–59.

Behnam Azad B, Banerjee SR, Pullambhatla M, Lacerda S, Foss CA, Wang Y*et al.* (2015). Evaluation of a PSMA-targeted BNF nanoparticle construct. Nanoscale 7: 4432–4442.

Berent-Spillson A, Robinson AM, Golovoy D, Slusher B, Rojas C, Russell JW (2004). Protection against glucose-induced neuronal death by NAAG and GCP II inhibition is regulated by mGluR3. J Neurochem 89: 90–99.

Bouchelouche K, Choyke PL, Capala J (2010). Prostate specific membrane antigen—a target for imaging and therapy with radionuclides. Discov Med 9: 55.

Bruno V, Battaglia G, Casabona G, Copani A, Caciagli F, Nicoletti F (1998). Neuroprotection by glial metabotropic glutamate receptors is mediated by transforming growth factor-β. J Neurosci 18: 9594–9600.

Cao Y, Gao Y, Xu S, Bao J, Lin Y, Luo X *et al.* (2016). Glutamate carboxypeptidase II gene knockout attenuates oxidative stress and cortical apoptosis after traumatic brain injury. BMC Neurosci 17: 1.

Ceci F, Uprimny C, Nilica B, Geraldo L, Kendler D, Kroiss A *et al.* (2015). 68Ga-PSMA PET/CT for restaging recurrent prostate cancer: which factors are associated with PET/CT detection rate? Eur J Nucl Med Mol Imaging 42: 1284–1294.

Chang SS, O'Keefe DS, Bacich DJ, Reuter VE, Heston WD, Gaudin PB (1999a). Prostate-specific membrane antigen is produced in tumor-associated neovasculature. Clin Cancer Res 5: 2674–2681.

Chang SS, Reuter VE, Heston W, Bander NH, Grauer LS, Gaudin PB (1999b). Five different anti-prostate-specific membrane antigen (PSMA) antibodies confirm PSMA expression in tumor-associated neovasculature. Cancer Res 59: 3192–3198.

Chang SS, Bander NH, Heston WD (2004). Biology of PSMA as a diagnostic and therapeutic target. In: Klein EA (ed.). Management of Prostate Cancer. Springer: Totowa, NJ, pp. 609–630.

Chang SS, Gaudin PB, Reuter VE, Heston WD (2000). Prostate-specific membrane antigen: present and future applications. Urology 55: 622–629.

Chatalic KL, Veldhoven-Zweistra J, Bolkestein M, Hoeben S, Koning GA, Boerman OC *et al.* (2015). A novel 111In-labeled anti-PSMA nanobody for targeted SPECT/CT imaging of prostate cancer. J Nucl Med 56: 1094–1099.

Chen R, Zhao Y, Huang Y, Yang Q, Zeng X, Jiang W*et al.* (2015). Nanomicellar TGX221 blocks xenograft tumor growth of prostate cancer in nude mice. Prostate 75: 593–602.

Chen S-R, Wozniak KM, Slusher BS, Pan H-L (2002). Effect of 2-(phosphono-methyl)-pentanedioic acid on allodynia and afferent ectopic discharges in a rat model of neuropathic pain. J Pharmacol Exp Ther 300: 662–667.

Chen Y, Pullambhatla M, Foss CA, Byun Y, Nimmagadda S, Senthamizhchelvan S *et al.* (2011). 2-(3-{1-Carboxy-5-[(6-[18F] fluoro-pyridine-3-carbonyl)-amino]-pentyl}-ureido)-pentanedioic acid, [18F] DCFPyL, a PSMA-based PET imaging agent for prostate cancer. Clin Cancer Res 17: 7645–7653.

Chen Y, Wang G, Kong D, Zhang Z, Yang K, Liu R *et al.* (2013). Double-targeted and double-enhanced suicide gene therapy mediated by generation 5 polyamidoamine dendrimers for prostate cancer. Mol Carcinog 52: 237–246.

Chen Z, Penet M-F, Nimmagadda S, Li C, Banerjee SR, Winnard PT Jr *et al.* (2012). PSMA-targeted theranostic nanoplex for prostate cancer therapy. ACS Nano 6: 7752–7762.

Cho SY, Gage KL, Mease RC, Senthamizhchelvan S, Holt DP, Jeffrey-Kwanisai A *et al.* (2012). Biodistribution, tumor detection, and radiation dosimetry of 18F-DCFBC, a low-molecular-weight inhibitor

of prostate-specific membrane antigen, in patients with metastatic prostate cancer. J Nucl Med 53: 1883–1891.

Choi J-Y, Kim J-H, Jo SA (2014). Acetylation regulates the stability of glutamate carboxypeptidase II protein in human astrocytes. Biochem Biophys Res Commun 450: 372–377.

Chu TC, Shieh F, Lavery LA, Levy M, Richards-Kortum R, Korgel BA *et al.* (2006). Labeling tumor cells with fluorescent nanocrystal–aptamer bioconjugates. Biosens Bioelectron 21: 1859–1866.

Conway RE, Joiner K, Patterson A, Bourgeois D, Rampp R, Hannah BC *et al.* (2013). Prostate specific membrane antigen produces pro-angiogenic laminin peptides downstream of matrix metalloprotease-2. Angiogenesis 16: 847–860.

Conway RE, Petrovic N, Li Z, Heston W, Wu D, Shapiro LH (2006). Prostate-specific membrane antigen regulates angiogenesis by modulating integrin signal transduction. Mol Cell Biol 26: 5310–5324.

Cooperberg MR, Broering JM, Carroll PR (2010). Time trends and local variation in primary treatment of localized prostate cancer. J Clin Oncol 28: 1117–1123.

Coyle JT (1997). The nagging question of the function of N-acetylaspartylglutamate. Neurobiol Dis 4: 231–238.

Dachs GU, Tupper J, Tozer GM (2005). From bench to bedside for gene-directed enzyme prodrug therapy of cancer. Anticancer Drugs 16: 349–359.

Dassie JP, Hernandez LI, Thomas GS, Long ME, Rockey WM, Howell CA *et al.* (2014). Targeted inhibition of prostate cancer metastases with an RNA aptamer to prostate-specific membrane antigen. Mol Ther 22: 1910–1922.

Dassie JP, X-y L, Thomas GS, Whitaker RM, Thiel KW, Stockdale KR *et al.* (2009). Systemic administration of optimized aptamer-siRNA chimeras promotes regression of PSMA-expressing tumors. Nat Biotechnol 27: 839–846.

Davis MI, Bennett MJ, Thomas LM, Bjorkman PJ (2005). Crystal structure of prostate-specific membrane antigen, a tumor marker and peptidase. Proc Natl Acad Sci 102: 5981–5986.

De la Vieja A, Dohan O, Levy O, Carrasco N (2000). Molecular analysis of the sodium/iodide symporter: impact on thyroid and extrathyroid pathophysiology. Physiol Rev 80: 1083–1105.

Deb N, Goris M, Trisler K, Fowler S, Saal J, Ning S *et al.* (1996). Treatment of hormone-refractory prostate cancer with 90Y-CYT-356 monoclonal antibody. Clin Cancer Res 2: 1289–1297.

Delaney G, Jacob S, Featherstone C, Barton M (2006). The role of radiotherapy in cancer treatment: estimating optimal utilisation from a review of evidence-based guidelines. Cancer 104: 1129–1137.

Demirkol MO, Acar Ö, Uçar B, Ramazanoğlu SR, Sağlıcan Y, Esen T (2015). Prostate-specific membrane antigen-based imaging in prostate cancer: Impact on clinical decision making process. Prostate 75: 748–757.

Denmeade SR, Mhaka AM, Rosen DM, Brennen WN, Dalrymple S, Dach I *et al.* (2012). Engineering a prostate-specific membrane antigen–activated tumor endothelial cell prodrug for cancer therapy. Sci Transl Med 4: 140ra186–140ra186.

Dhar S, Kolishetti N, Lippard SJ, Farokhzad OC (2011). Targeted delivery of a cisplatin prodrug for safer and more effective prostate cancer therapy in vivo. Proc Natl Acad Sci 108: 1850–1855.

Dietlein M, Kobe C, Kuhnert G, Stockter S, Fischer T, Schomäcker K *et al.* (2015). Comparison of [18F] DCFPyL and [68Ga] Ga-PSMA-HBED-CC for PSMA-PET imaging in patients with relapsed prostate cancer. Mol Imaging Biol 17: 575–584.

DiPippo VA, Olson WC, Nguyen HM, Brown LG, Vessella RL, Corey E (2015). Efficacy studies of an antibody-drug conjugate PSMA-ADC in patient-derived prostate cancer xenografts. Prostate 75: 303–313.

Donovan JL (2012). Presenting treatment options to men with clinically localized prostate cancer: the acceptability of active surveillance/monitoring. J Natl Cancer Inst Monogr 2012: 191.

Du Y-F, Long Q-Z, Shi Y, Liu X-G, Li X-D, Zeng J *et al.* (2013). Prostate-targeted mTOR-shRNA inhibit prostate cancer cell growth in human tumor xenografts. Int J Clin Exp Med 6: 126.

Eder M, Schäfer M, Bauder-Wüst U, Haberkorn U, Eisenhut M, Kopka K (2014). Preclinical evaluation of a bispecific low-molecular heterodimer targeting both PSMA and GRPR for improved PET imaging and therapy of prostate cancer. Prostate 74: 659–668.

Eiber M, Maurer T, Souvatzoglou M, Beer AJ, Ruffani A, Haller B *et al.* (2015). Evaluation of Hybrid 68Ga-PSMA Ligand PET/CT in 248 patients with biochemical recurrence after radical prostatectomy. J Nucl Med 56: 668–674.

Eshhar Z (2008). The T-body approach: redirecting T cells with antibody specificity. In: Chernajovsky Y, Nissim A (eds). Therapeutic Antibodies. Springer: Berlin Heidelberg, pp. 329–342.

Etzioni R, Penson DF, Legler JM, di Tommaso D, Boer R, Gann PH *et al.* (2002). Overdiagnosis due to prostate-specific antigen screening: lessons from US prostate cancer incidence trends. J Natl Cancer Inst 94: 981–990.

Evans J, McCarthy J, Torres-Fuentes C, Cryan J, Ogier J, Darcy R *et al.* (2015). Cyclodextrin mediated delivery of NF-κB and SRF siRNA reduces the invasion potential of prostate cancer cells in vitro. Gene Ther 22: 802–810.

Fan X, Wang L, Guo Y, Tu Z, Li L, Tong H *et al.* (2015). Ultrasonic Nanobubbles carrying anti-psma nanobody: construction and application in prostate cancer-targeted imaging. PLoS One 10: e0127419.

Feng J-F, Van KC, Gurkoff GG, Kopriva C, Olszewski RT, Song M *et al.* (2011). Post-injury administration of NAAG peptidase inhibitor prodrug, PGI-02776, in experimental TBI. Brain Res 1395: 62–73.

Ferraris DV, Shukla K, Tsukamoto T (2012). Structure–activity relationships of glutamate carboxypeptidase II (GCPII) inhibitors. Curr Med Chem 19: 1282–1294.

Ferraro B, Cisper NJ, Talbott KT, Philipson-Weiner L, Lucke CE, Khan AS *et al.* (2011). Co-delivery of PSA and PSMA DNA vaccines with electroporation induces potent immune responses. Hum Vaccin 7 (Supp1): 120–127.

Fishman M (2009). A changing world for DCvax: a PSMA loaded autologous dendritic cell vaccine for prostate cancer. Expert Opin Biol Ther 9: 1565–1575.

Rahn KA, Slusher BS, Kaplin AI (2012). Glutamate in CNS neurodegeneration and cognition and its regulation by GCPII inhibition. Curr Med Chem 19: 1335–1345.

Fortmüller K, Alt K, Gierschner D, Wolf P, Baum V, Freudenberg N *et al.* (2011). Effective targeting of prostate cancer by lymphocytes redirected by a PSMA× CD3 bispecific single-chain diabody. Prostate 71: 588–596.

Fuessel S, Meye A, Schmitz M, Zastrow S, Linné C, Richter K *et al.* (2006). Vaccination of hormone-refractory prostate cancer patients with peptide cocktail-loaded dendritic cells: Results of a phase I clinical trial. Prostate 66: 811–821.

Ganguly T, Dannoon S, Hopkins MR, Murphy S, Cahaya H, Blecha JE *et al.* (2015). A high-affinity [18 F]-labeled phosphoramidate peptidomimetic PSMA-targeted inhibitor for PET imaging of prostate cancer. Nucl Med Biol 42: 780–787.

Gao X-F, Zhou T, Chen G-H, Xu C-L, Ding Y-L, Sun Y-H (2014). Radioiodine therapy for castration-resistant prostate cancer following prostate-specific membrane antigen promoter-mediated transfer of the human sodium iodide symporter. Asian J Androl 16: 120.

Ghadge GD, Slusher BS, Bodner A, Dal Canto M, Wozniak K, Thomas AG *et al.* (2003). Glutamate carboxypeptidase II inhibition protects motor neurons from death in familial amyotrophic lateral sclerosis models. Proc Natl Acad Sci 100: 9554–9559.

Ghosh A, Heston WD (2005a). Understanding prostate-specific membrane antigen and its implication in prostate cancer. In: LaRochelle WJ, Shimkets RA (eds). The Oncogenomics Handbook. Springer: Totowa, NJ, pp. 597–615.

Ghosh A, Wang X, Klein E, Heston WD (2005b). Novel role of prostate-specific membrane antigen in suppressing prostate cancer invasiveness. Cancer Res 65: 727–731.

Giesel FL, Fiedler H, Stefanova M, Sterzing F, Rius M, Kopka K *et al.* (2015). PSMA PET/CT with Glu-urea-Lys-(Ahx)-[68Ga (HBED-CC)] versus 3D CT volumetric lymph node assessment in recurrent prostate cancer. Eur J Nucl Med Mol Imaging 42: 1794–1800.

Goodman OB, Barwe SP, Ritter B, McPherson PS, Vasko A-J, Keen JH *et al.* (2007). Interaction of prostate specific membrane antigen with clathrin and the adaptor protein complex-2. Int J Oncol 31: 1199–1203.

Graham K, Lesche R, Gromov AV, Böhnke N, Schäfer M, Hassfeld J *et al.* (2012). Radiofluorinated derivatives of 2-(Phosphonomethyl) pentanedioic acid as inhibitors of prostate specific membrane antigen (PSMA) for the imaging of prostate cancer. J Med Chem 55: 9510–9520.

Grimm D, Kay MA (2007). RNAi and gene therapy: a mutual attraction. Hematology Am Soc Hematol Educ Program 2007: 473–481.

Grupp SA, Kalos M, Barrett D, Aplenc R, Porter DL, Rheingold SR *et al.* (2013). Chimeric antigen receptor–modified T cells for acute lymphoid leukemia. N Engl J Med 368: 1509–1518.

Guilarte TR, Hammoud DA, McGlothan JL, Caffo BS, Foss CA, Kozikowski AP *et al.* (2008). Dysregulation of glutamate carboxypeptidase II in psychiatric disease. Schizophr Res 99: 324–332.

Guilarte TR, McGlothan JL, Foss CA, Zhou J, Heston WD, Kozikowski AP *et al.* (2005). Glutamate carboxypeptidase II levels in rodent brain using [125 I] DCIT quantitative autoradiography. Neurosci Lett 387: 141–144.

Guo H, Liu J, Van Shura K, Chen H, Flora MN, Myers TM *et al.* (2015). N-acetyl-aspartyl-glutamate and inhibition of glutamate carboxypeptidases protects against soman-induced neuropathology. Neurotoxicology 48: 180–191.

Guo J, Evans JC, O'Driscoll CM (2013a). Delivering RNAi therapeutics with non-viral technology: a promising strategy for prostate cancer? Trends Mol Med 19: 250–261.

Guo Z, Huang H, Zeng L, Du T, Xu K, Lin T*et al.* (2011). Lentivirus-mediated RNAi knockdown of prostate-specific membrane antigen suppresses growth, reduces migration ability and the invasiveness of prostate cancer cells. Med Oncol 28: 878–887.

Guo Z, Lai Y, Zhang Y, Chen J, Bi L, Lin T*et al.* (2013b). Prostate specific membrane antigen knockdown impairs the tumorigenicity of LNCaP prostate cancer cells by inhibiting the phosphatidylinositol 3-kinase/Akt signaling pathway. Chin Med J (Engl) 127: 929–936.

Gurkoff GG, Feng J-F, Van KC, Izadi A, Ghiasvand R, Shahlaie K *et al.* (2013). NAAG peptidase inhibitor improves motor function and reduces cognitive dysfunction in a model of TBI with secondary hypoxia. Brain Res 1515: 98–107.

Haffner MC, Kronberger IE, Ross JS, Sheehan CE, Zitt M, Mühlmann G *et al.* (2009). Prostate-specific membrane antigen expression in the neovasculature of gastric and colorectal cancers. Hum Pathol 40: 1754–1761.

Hao Z, Fan W, Hao J, Wu X, Zeng GQ, Zhang LJ *et al.* (2016). Efficient delivery of micro RNA to bone-metastatic prostate tumors by using aptamer-conjugated atelocollagen in vitro and in vivo. Drug Deliv 23: 864–871.

Hariri W, Sudha T, Bharali DJ, Cui H, Mousa SA (2015). Nano-targeted delivery of toremifene, an estrogen receptor-α blocker in prostate cancer. Pharm Res 32: 2764–2774.

Hillier SM, Maresca KP, Lu G, Merkin RD, Marquis JC, Zimmerman CN *et al.* (2013). 99mTc-labeled small-molecule inhibitors of prostate-specific membrane antigen for molecular imaging of prostate cancer. J Nucl Med 54: 1369–1376.

Hlouchová K, Bařinka C, Klusák V, Šácha P, Mlčochová P, Majer P *et al.* (2007). Biochemical characterization of human glutamate carboxypeptidase III. J Neurochem 101: 682–696.

Horoszewicz JS, Kawinski E, Murphy G (1986). Monoclonal antibodies to a new antigenic marker in epithelial prostatic cells and serum of prostatic cancer patients. Anticancer Res 7: 927–935.

Hrkach J, Von Hoff D, Ali MM, Andrianova E, Auer J, Campbell T*et al.* (2012). Preclinical development and clinical translation of a PSMA-targeted docetaxel nanoparticle with a differentiated pharmacological profile. Sci Transl Med 4: 128ra139–128ra139.

Huang B, Otis J, Joice M, Kotlyar A, Thomas TP (2014). PSMA-targeted stably linked "dendrimer-glutamate urea-methotrexate" as a prostate cancer therapeutic. Biomacromolecules 15: 915–923.

Israeli RS, Powell CT, Fair WR, Heston WD (1993). Molecular cloning of a complementary DNA encoding a prostate-specific membrane antigen. Cancer Res 53: 227–230.

Jackson AL, Linsley PS (2010). Recognizing and avoiding siRNA off-target effects for target identification and therapeutic application. Nat Rev Drug Discov 9: 57–67.

Jackson PF, Cole DC, Slusher BS, Stetz SL, Ross LE, Donzanti BA *et al.* (1996). Design, synthesis, and biological activity of a potent inhibitor of the neuropeptidase N-acetylated α-linked acidic dipeptidase. J Med Chem 39: 619–622.

Jackson SP, Bartek J (2009). The DNA-damage response in human biology and disease. Nature 461: 1071–1078.

Janczura KJ, Olszewski RT, Bzdega T, Bacich DJ, Heston WD, Neale JH (2013). NAAG peptidase inhibitors and deletion of NAAG peptidase gene enhance memory in novel object recognition test. Eur J Pharmacol 701: 27–32.

Jin J, Sui B, Gou J, Liu J, Tang X, Xu H *et al.* (2014). PSMA ligand conjugated PCL-PEG polymeric micelles targeted to prostate cancer cells.

Kahn D, Austin JC, Maguire RT, Miller SJ, Gerstbrein J, Williams RD (1999). A phase II study of [90Y] yttrium-capromab pendetide in the treatment of men with prostate cancer recurrence following radical prostatectomy. Cancer Biother Radiopharm 14: 99–111.

Kahn D, Williams RD, Haseman MK, Reed NL, Miller SJ, Gerstbrein J (1998a). Radioimmunoscintigraphy with In-111-labeled capromab pendetide predicts prostate cancer response to salvage radiotherapy after failed radical prostatectomy. J Clin Oncol 16: 284–289.

Kahn D, Williams RD, Manyak MJ, Haseman MK, Seldin DW, Libertino JA *et al.* (1998b). (111) Indium-capromab pendetide in the evaluation of patients with residual or recurrent prostate cancer after radical prostatectomy. J Urol 159: 2041–2047.

Kampmeier F, Williams JD, Maher J, Mullen GE, Blower PJ (2014). Design and preclinical evaluation of a 99mTc-labelled diabody of mAb J591 for SPECT imaging of prostate-specific membrane antigen (PSMA). EJNMMI Res 4: 13.

Kawabata H, Yang R, Hirama T, Vuong PT, Kawano S, Gombart AF *et al.* (1999). Molecular cloning of transferrin receptor 2 A new member of the transferrin receptor-like family. J Biol Chem 274: 20826–20832.

Khacho P, Wang B, Ahlskog N, Hristova E, Bergeron R (2015). Differential effects of N-acetyl-aspartyl-glutamate on synaptic and extrasynaptic NMDA receptors are subunit-and pH-dependent in the CA1 region of the mouse hippocampus. Neurobiol Dis 82: 580–592.

Kiess A, Minn I, Chen Y, Hobbs RF, Sgouros G, Mease RC *et al.* (2015). Auger radiopharmaceutical therapy targeting prostate-specific membrane antigen. J Nucl Med 56: 1401–1407.

Kim E, Jung Y, Choi H, Yang J, Suh J-S, Huh Y-M *et al.* (2010). Prostate cancer cell death produced by the co-delivery of Bcl-xL shRNA and doxorubicin using an aptamer-conjugated polyplex. Biomaterials 31: 4592–4599.

Kim JS, Lee SD, Lee SJ, Chung MK (2013). Development of an immunotherapeutic adenovirus targeting hormone-independent prostate cancer. OncoTargets Ther 6: 1635.

Kozikowski AP, Nan F, Conti P, Zhang J, Ramadan E, Bzdega T*et al.* (2001). Design of remarkably simple, yet potent urea-based inhibitors of glutamate carboxypeptidase II (NAALADase)[1]. J Med Chem 44: 298–301.

Kozikowski AP, Zhang J, Nan F, Petukhov PA, Grajkowska E, Wroblewski JT*et al.* (2004). Synthesis of urea-based inhibitors as active site probes of glutamate carboxypeptidase II: efficacy as analgesic agents. J Med Chem 47: 1729–1738.

Kratochwil C, Giesel FL, Eder M, Afshar-Oromieh A, Benešová M, Mier W*et al.* (2015). [177Lu] Lutetium-labelled PSMA ligand-induced remission in a patient with metastatic prostate cancer. Eur J Nucl Med Mol Imaging 42: 987–988.

Krop IE, Beeram M, Modi S, Jones SF, Holden SN, Yu W*et al.* (2010). Phase I study of trastuzumab-DM1, an HER2 antibody-drug conjugate, given every 3 weeks to patients with HER2-positive metastatic breast cancer. J Clin Oncol 28: 2698–2704.

Larson SM, Carrasquillo JA, Cheung N-KV, Press OW (2015). Radioimmunotherapy of human tumours. Nat Rev Cancer 15: 347–360.

Lawrence CM, Ray S, Babyonyshev M, Galluser R, Borhani DW, Harrison SC (1999). Crystal structure of the ectodomain of human transferrin receptor. Science 286: 779–782.

Lee I-H, An S, Yu MK, Kwon H-K, Im S-H, Jon S (2011). Targeted chemoimmunotherapy using drug-loaded aptamer–dendrimer bioconjugates. J Control Release 155: 435–441.

Lesche R, Kettschau G, Gromov AV, Böhnke N, Borkowski S, Mönning U *et al.* (2014). Preclinical evaluation of BAY 1075553, a novel 18F-labelled inhibitor of prostate-specific membrane antigen for PET imaging of prostate cancer. Eur J Nucl Med Mol Imaging 41: 89–101.

Lodder-Gadaczek J, Becker I, Gieselmann V, Wang-Eckhardt L, Eckhardt M (2011). N-acetylaspartylglutamate synthetase II synthesizes N-acetylaspartylglutamylglutamate. J Biol Chem 286: 16693–16706.

Lonergan PE, Tindall DJ (2011). Androgen receptor signaling in prostate cancer development and progression. J Carcinog 10: 20.

Long JB, Yourick DL, Slusher BS, Robinson MB, Meyerhoff JL (2005). Inhibition of glutamate carboxypeptidase II (NAALADase) protects against dynorphin A-induced ischemic spinal cord injury in rats. Eur J Pharmacol 508: 115–122.

Łukawski K, Kamiński RM, Czuczwar SJ (2008). Effects of selective inhibition of N-acetylated-α-linked-acidic dipeptidase (NAALADase) on mice in learning and memory tasks. Eur J Pharmacol 579: 202–207.

Luthi-Carter R, Barczak AK, Speno H, Coyle JT (1998). Hydrolysis of the neuropeptide N-acetylaspartylglutamate (NAAG) by cloned human glutamate carboxypeptidase II. Brain Res 795: 341–348.

Lütje S, Rijpkema M, Franssen GM, Fracasso G, Helfrich W, Eek A *et al.* (2014). Dual-modality image-guided surgery of prostate cancer with a radiolabeled fluorescent anti-PSMA monoclonal antibody. J Nucl Med 55: 995–1001.

Ma Q, Gomes EM, Lo ASY, Junghans RP (2014). Advanced generation anti-prostate specific membrane antigen designer T Cells for prostate cancer immunotherapy. Prostate 74: 286–296.

Mahadevan D, Saldanha JW (1999). The extracellular regions of PSMA and the transferrin receptor contain an aminopeptidase domain: implications for drug design. Protein Sci 8: 2546–2549.

Majer P, Jackson PF, Delahanty G, Grella BS, Ko Y-S, Li W*et al.* (2003). Synthesis and biological evaluation of thiol-based inhibitors of glutamate carboxypeptidase II: discovery of an orally active GCP II inhibitor. J Med Chem 46: 1989–1996.

Majer P, Jančařík A, Krecmerova M, Tichý TS, Tenora LS, Wozniak K *et al.* (2016). Discovery of orally available prodrugs of the glutamate carboxypeptidase II (GCPII) inhibitor 2-phosphonomethylpentanedioic acid (2-PMPA). J Med Chem 59: 2810–2819.

Martin SE, Ganguly T, Munske GR, Fulton MD, Hopkins MR, Berkman CE *et al.* (2014). Development of inhibitor-directed enzyme prodrug therapy (IDEPT) for prostate cancer. Bioconjug Chem 25: 1752–1760.

Mazzaferri EL, Kloos R (1996). Carcinoma of follicular epithelium: radioiodine and other treatments and outcomes. In: Braverman LE, Utiger RD (eds). The Thyroid: A Fundamental and Clinical Text, Vol. 7. Philadelphia, PA, pp. 922–945.

McKinzie D, Li TK, McBride W, Slusher B (2000). NAALADase inhibition reduces alcohol consumption in the alcohol-preferring (P) line of rats. Addict Biol 5: 411–416.

Mesters JR, Barinka C, Li W, Tsukamoto T, Majer P, Slusher BS *et al.* (2006). Structure of glutamate carboxypeptidase II, a drug target in neuronal damage and prostate cancer. EMBO J 25: 1375–1384.

Milowsky MI, Nanus DM, Kostakoglu L, Sheehan CE, Vallabhajosula S, Goldsmith SJ *et al.* (2007). Vascular targeted therapy with anti–prostate-specific membrane antigen monoclonal antibody J591 in advanced solid tumors. J Clin Oncol 25: 540–547.

Morigi JJ, Stricker P, Van Leeuwen P, Tang R, Ho B, Nguyen Q *et al.* (2015). Prospective Comparison of the detection rate of18F-Fluoromethylcholine and 68Ga-PSMA-HBED PET/CT in men with

prostate cancer with rising PSA post curative treatment, being considered for targeted therapy. J Nucl Med 56: 1185–1190.

Morris MJ, Pandit-Taskar N, Divgi CR, Bender S, O'Donoghue JA, Nacca A *et al.* (2007). Phase I evaluation of J591 as a vascular targeting agent in progressive solid tumors. Clin Cancer Res 13: 2707–2713.

Nagel J, Belozertseva I, Greco S, Kashkin V, Malyshkin A, Jirgensons A *et al.* (2006). Effects of NAAG peptidase inhibitor 2-PMPA in model chronic pain–relation to brain concentration. Neuropharmacology 51: 1163–1171.

Nan F, Bzdega T, Pshenichkin S, Wroblewski JT, Wroblewska B, Neale JH *et al.* (2000). Dual function glutamate-related ligands: discovery of a novel, potent inhibitor of glutamate carboxypeptidase II possessing mGluR3 agonist activity. J Med Chem 43: 772–774.

Navrátil M, Ptáček J, Šácha P, Starková J, Lubkowski J, Bařinka C *et al.* (2014). Structural and biochemical characterization of the folyl-poly-γ-l-glutamate hydrolyzing activity of human glutamate carboxypeptidase II. FEBS J 281: 3228–3242.

Navrátil M, Tykvart J, Schimer J, Pachl P, Navrátil V, Rokob TA *et al.* (2016). Comparison of human glutamate carboxypeptidases II and III reveals their divergent substrate specificities. FEBS J 283: 2528–2545.

Neale JH, Bzdega T, Wroblewska B (2000). N-Acetylaspartylglutamate: the most abundant peptide neurotransmitter in the mammalian central nervous system. J Neurochem 75: 443–452.

Neale JH, Olszewski RT, Zuo D, Janczura KJ, Profaci CP, Lavin KM *et al.* (2011). Advances in understanding the peptide neurotransmitter NAAG and appearance of a new member of the NAAG neuropeptide family. J Neurochem 118: 490–498.

Ni X, Zhang Y, Ribas J, Chowdhury WH, Castanares M, Zhang Z *et al.* (2011). Prostate-targeted radiosensitization via aptamer-shRNA chimeras in human tumor xenografts. J Clin Invest 121: 2383.

Nomura N, Pastorino S, Jiang P, Lambert G, Crawford JR, Gymnopoulos M *et al.* (2014). Prostate specific membrane antigen (PSMA) expression in primary gliomas and breast cancer brain metastases. Cancer Cell Int 14: 26.

O'donoghue J, Bardies M, Wheldon T (1995). Relationships between tumor size and curability for uniformly targeted therapy with beta-emitting radionuclides. J Nucl Med 36: 1902–1909.

O'Keefe DS, Uchida A, Bacich DJ, Watt FB, Martorana A, Molloy PL *et al.* (2000). Prostate-specific suicide gene therapy using the prostate-specific membrane antigen promoter and enhancer. Prostate 45: 149–157.

O'Keefe DS, Su SL, Bacich DJ, Horiguchi Y, Luo Y, Powell CT*et al.* (1998). Mapping, genomic organization and promoter analysis of the human prostate-specific membrane antigen gene. Biochim Biophys Acta Gene Struct Expression 1443: 113–127.

Olszewski R, Janczura K, Ball S, Madore J, Lavin K, Lee JC *et al.* (2012). NAAG peptidase inhibitors block cognitive deficit induced by MK-801 and motor activation induced by d-amphetamine in animal models of schizophrenia. Transl Psychiatry 2: e145.

Olszewski RT, Bukhari N, Zhou J, Kozikowski AP, Wroblewski JT, Shamimi-Noori S *et al.* (2004). NAAG peptidase inhibition reduces locomotor activity and some stereotypes in the PCP model of schizophrenia via group II mGluR. J Neurochem 89: 876–885.

Osborne JR, Akhtar NH, Vallabhajosula S, Anand A, Deh K, Tagawa ST (2013). Prostate-specific membrane antigen-based imaging. Urol Oncol 31: 144–154.

Oser MG, Niederst MJ, Sequist LV, Engelman JA (2015). Transformation from non-small-cell lung cancer to small-cell lung cancer: molecular drivers and cells of origin. Lancet Oncol 16: e165–e172.

Palucka K, Banchereau J (2012). Cancer immunotherapy via dendritic cells. Nat Rev Cancer 12: 265–277.

Pandit-Taskar N, O'Donoghue JA, Durack JC, Lyashchenko SK, Cheal SM, Beylergil V*et al.* (2015a). A phase I/II study for analytic validation of 89Zr-J591 immunoPET as a molecular imaging agent for metastatic prostate cancer. Clin Cancer Res 21: 5277–5285.

Pandit-Taskar N, O'Donoghue JA, Divgi CR, Wills EA, Schwartz L, Gönen M *et al.* (2015b). Indium 111-labeled J591 anti-PSMA antibody for vascular targeted imaging in progressive solid tumors. EJNMMI Res 5: 1–13.

Pangalos MN, Neefs J-M, Somers M, Verhasselt P, Bekkers M, van der Helm L *et al.* (1999). Isolation and expression of novel human glutamate carboxypeptidases with N-acetylated α-linked acidic dipeptidase and dipeptidyl peptidase IV activity. J Biol Chem 274: 8470–8483.

Peng Z-H, Sima M, Salama ME, Kopečková P, Kopeček J (2013). Spacer length impacts the efficacy of targeted docetaxel conjugates in prostate-specific membrane antigen expressing prostate cancer. J Drug Target 21: 968–980.

Pérez-Herrero E, Fernández-Medarde A (2015). Advanced targeted therapies in cancer: drug nanocarriers, the future of chemotherapy. Eur J Pharm Biopharm 93: 52–79.

Pienta KJ, Bradley D (2006). Mechanisms underlying the development of androgen-independent prostate cancer. Clin Cancer Res 12: 1665–1671.

Pinto JT, Suffoletto BP, Berzin TM, Qiao CH, Lin S, Tong WP *et al.* (1996). Prostate-specific membrane antigen: a novel folate hydrolase in human prostatic carcinoma cells. Clin Cancer Res 2: 1445–1451.

Pomper MG, Musachio JL, Zhang J, Scheffel U, Zhou Y, Hilton J *et al.* (2002). 11C-MCG: synthesis, uptake selectivity, and primate PET of a probe for glutamate carboxypeptidase II (NAALADase). Mol Imaging 1: 96–101.

Porter DL, Levine BL, Kalos M, Bagg A, June CH (2011). Chimeric antigen receptor–modified T cells in chronic lymphoid leukemia. N Engl J Med 365: 725–733.

Potter MC, Wozniak KM, Callizot N, Slusher BS (2014). Glutamate carboxypeptidase II inhibition behaviorally and physiologically improves pyridoxine-induced neuropathy in rats. PLoS One 9: e102936.

Profaci CP, Krolikowski KA, Olszewski RT, Neale JH (2011). Group II mGluR agonist LY354740 and NAAG peptidase inhibitor effects on prepulse inhibition in PCP and D-amphetamine models of schizophrenia. Psychopharmacology (Berl) 216: 235–243.

Rais R, Wozniak K, Wu Y, Niwa M, Stathis M, Alt J *et al.* (2015). Selective CNS uptake of the GCP-II inhibitor 2-PMPA following intranasal administration. PLoS One 10: e0131861.

Rajasekaran SA, Anilkumar G, Oshima E, Bowie JU, Liu H, Heston W *et al.* (2003). A novel cytoplasmic tail MXXXL motif mediates the internalization of prostate-specific membrane antigen. Mol Biol Cell 14: 4835–4845.

Ray Banerjee S, Pullambhatla M, Foss CA, Falk A, Byun Y, Nimmagadda S *et al.* (2013). Effect of chelators on the pharmacokinetics of 99mTc-labeled imaging agents for the prostate-specific membrane antigen (PSMA). J Med Chem 56: 6108–6121.

Ren H, Zhang H, Wang X, Liu J, Yuan Z, Hao J (2014). Prostate-specific membrane antigen as a marker of pancreatic cancer cells. Med Oncol 31: 1–6.

Resnick MJ, Koyama T, Fan K-H, Albertsen PC, Goodman M, Hamilton AS *et al.* (2013). Long-term functional outcomes after treatment for localized prostate cancer. N Engl J Med 368: 436–445.

Riveros N, Orrego F (1984). A study of possible excitatory effects of N-acetylaspartylglutamate in different in vivo and in vitro brain preparations. Brain Res 299: 393–395.

Robbins HA, Pfeiffer RM, Shiels MS, Li J, Hall HI, Engels EA (2015). Excess cancers among HIV-infected people in the United States. J Natl Cancer Inst 107: dju503.

Robinson MB, Blakely R, Couto R, Coyle J (1987). Hydrolysis of the brain dipeptide N-acetyl-L-aspartyl-L-glutamate. Identification and characterization of a novel N-acetylated alpha-linked acidic dipeptidase activity from rat brain. J Biol Chem 262: 14498–14506.

Romei C, Raiteri M, Raiteri L (2013). Glycine release is regulated by metabotropic glutamate receptors sensitive to mGluR2/3 ligands and activated by N-acetylaspartylglutamate (NAAG). Neuropharmacology 66: 311–316.

Rowdo FPM, Baron A, Urrutia M, Mordoh J (2015). Immunotherapy in cancer: a combat between tumors and the immune system; you win some, you lose some. Front Immunol 6: 127.

Rowe SP, Gage KL, Faraj SF, Macura KJ, Cornish TC, Gonzalez-Roibon N *et al.* (2015). 18F-DCFBC PET/CT for PSMA-based detection and characterization of primary prostate cancer. J Nucl Med 56: 1003–1010.

Roy J, Nguyen TX, Kanduluru AK, Venkatesh C, Lv W, Reddy PN *et al.* (2015). DUPA conjugation of a cytotoxic indenoisoquinoline topoisomerase i inhibitor for selective prostate cancer cell targeting. J Med Chem 58: 3094–3103.

Ruggiero A, Holland JP, Hudolin T, Shenker L, Koulova A, Bander NH *et al.* (2011). Targeting the internal epitope of prostate-specific membrane antigen with 89Zr-7E11 immuno-PET. J Nucl Med 52: 1608–1615.

Šácha P, Zámečník J, Bařinka C, Hlouchova K, Vicha A, Mlčochová P *et al.* (2007). Expression of glutamate carboxypeptidase II in human brain. Neuroscience 144: 1361–1372.

Samplaski MK, Heston W, Elson P, Magi-Galluzzi C, Hansel DE (2011). Folate hydrolase (prostate-specific antigen) 1 expression in bladder cancer subtypes and associated tumor neovasculature. Mod Pathol 24: 1521–1529.

Sanabria ERG, Wozniak KM, Slusher BS, Keller A (2004). GCP II (NAALADase) inhibition suppresses mossy fiber-CA3 synaptic neurotransmission by a presynaptic mechanism. J Neurophysiol 91: 182–193.

Sanna V, Pintus G, Roggio AM, Punzoni S, Posadino AM, Arca A *et al.* (2011). Targeted biocompatible nanoparticles for the delivery of (−)-epigallocatechin 3-gallate to prostate cancer cells. J Med Chem 54: 1321–1332.

Santoro S, Kim S, Motz G, Alatzoglou D, Li C, Irving M *et al.* (2014). T cells bearing a chimeric antigen receptor against prostate-specific membrane antigen mediate vascular disruption and result in tumor regression. Cancer Immunol Res 3: 68–84.

Schäfer M, Bauder-Wüst U, Leotta K, Zoller F, Mier W, Haberkorn U *et al.* (2012). A dimerized urea-based inhibitor of the prostate-specific membrane antigen for 68Ga-PET imaging of prostate cancer. EJNMMI Res 2: 23.

Schiavina R, Ceci F, Romagnoli D, Uprimny C, Brunocilla E, Borghesi M *et al.* (2015). 68 Ga-PSMA PET/CT-guided salvage retroperitoneal lymph node dissection for disease relapse after radical prostatectomy for prostate cancer. Clin Genitourin Cancer 13: e415–e417.

Schwenck J, Tabatabai G, Skardelly M, Reischl G, Beschorner R, Pichler B *et al.* (2015). In vivo visualization of prostate-specific membrane antigen in glioblastoma. Eur J Nucl Med Mol Imaging 42: 170–171.

Shafizadeh TB, Halsted CH (2007). γ-Glutamyl hydrolase, not glutamate carboxypeptidase II, hydrolyzes dietary folate in rat small intestine. J Nutr 137: 1149–1153.

Shallal HM, Minn I, Banerjee SR, Lisok A, Mease RC, Pomper MG (2014). Heterobivalent Agents Targeting PSMA and Integrin-αvβ3. Bioconjug Chem 25: 393–405.

Shippenberg TS, Rea W, Slusher BS (2000). Modulation of behavioral sensitization to cocaine by NAALADase inhibition. Synapse 38: 161–166.

Shuba Y, Prevarskaya N, Lemonnier L, Van Coppenolle F, Kostyuk P, Mauroy B *et al.* (2000). Volume-regulated chloride conductance in the LNCaP human prostate cancer cell line. Am J Physiol Cell Physiol 279: C1144–C1154.

Simone CB, Hahn SM (2013). What's in a Label? Radioimmunotherapy for Metastatic Prostate Cancer. Clin Cancer Res 19: 4908–4910.

Slusher BS, Thomas A, Paul M, Schad CA, Ashby CR (2001). Expression and acquisition of the conditioned place preference response to cocaine in rats is blocked by selective inhibitors of the enzyme N-acetylated-α-linked-acidic dipeptidase (NAALADASE). Synapse 41: 22–28.

Slusher BS, Vornov JJ, Thomas AG, Hurn PD, Harukuni I, Bhardwaj A *et al.* (1999). Selective inhibition of NAALADase, which converts NAAG to glutamate, reduces ischemic brain injury. Nat Med 5: 1396–1402.

Smith-Jones PM, Vallabahajosula S, Goldsmith SJ, Navarro V, Hunter CJ, Bastidas D *et al.* (2000). In vitro characterization of radiolabeled monoclonal antibodies specific for the extracellular domain of prostate-specific membrane antigen. Cancer Res 60: 5237–5243.

Southan C, Sharman JL, Benson HE, Faccenda E, Pawson AJ, Alexander SP *et al.* (2016). The IUPHAR/BPS guide to pHARMACOLOGY in 2016: towards curated quantitative interactions between 1300 protein targets and 6000 ligands. Nucleic Acids Res 44: D1054–D1068.

Strebhardt K, Ullrich A (2006). Targeting polo-like kinase 1 for cancer therapy. Nat Rev Cancer 6: 321–330.

Su Y, Yu L, Liu N, Guo Z, Wang G, Zheng J *et al.* (2013). PSMA specific single chain antibody-mediated targeted knockdown of Notch1 inhibits human prostate cancer cell proliferation and tumor growth. Cancer Lett 338: 282–291.

Sun H, Zhu X, Lu PY, Rosato RR, Tan W, Zu Y (2014a). Oligonucleotide aptamers: new tools for targeted cancer therapy. Mol Ther Nucleic Acids 3: e182.

Sun T, Zhang YS, Pang B, Hyun DC, Yang M, Xia Y (2014b). Engineered nanoparticles for drug delivery in cancer therapy. Angew Chem Int Ed 53: 12320–12364.

Sutradhar KB, Amin ML (2014). Nanotechnology in cancer drug delivery and selective targeting. ISRN Nanotechnol 2014. doi:10.1155/2014/939378.

Tagawa ST, Milowsky MI, Morris M, Vallabhajosula S, Christos P, Akhtar NH *et al.* (2013). Phase II Study of Lutetium-177–Labeled Anti-Prostate-Specific Membrane Antigen Monoclonal Antibody J591 for Metastatic Castration-Resistant Prostate Cancer. Clin Cancer Res 19: 5182–5191.

Taghdisi SM, Danesh NM, Sarreshtehdar Emrani A, Tabrizian K, ZandKarimi M, Ramezani M *et al.* (2013). Targeted delivery of Epirubicin to cancer cells by PEGylated A10 aptamer. J Drug Target 21: 739–744.

Takeshita F, Patrawala L, Osaki M, Takahashi R-U, Yamamoto Y, Kosaka N *et al.* (2010). Systemic delivery of synthetic microRNA-16 inhibits the growth of metastatic prostate tumors via downregulation of multiple cell-cycle genes. Mol Ther 18: 181–187.

Tallarida C, Song K, Raffa RB, Rawls SM (2012). Glutamate carboxypeptidase II (GCPII) inhibitor displays anti-glutamate and anti-cocaine effects in an invertebrate assay. Amino Acids 42: 2521–2524.

Tang L, Tong R, Coyle VJ, Yin Q, Pondenis H, Borst LB *et al.* (2015). Targeting tumor vasculature with aptamer-functionalized doxorubicin–polylactide nanoconjugates for enhanced cancer therapy. ACS Nano 9: 5072–5081.

Taylor RM, Huber DL, Monson TC, Ali A-MS, Bisoffi M, Sillerud LO (2011). Multifunctional iron platinum stealth immunomicelles: targeted detection of human prostate cancer cells using both fluorescence and magnetic resonance imaging. J Nanopart Res 13: 4717–4729.

Thakker D, Natt F, Huesken D, Van Der Putten H, Maier R, Hoyer D *et al.* (2005). siRNA-mediated knockdown of the serotonin transporter in the adult mouse brain. Mol Psychiatry 10: 782–789.

Thariat J, Hannoun-Levi J-M, Myint AS, Vuong T, Gérard J-P (2013). Past, present, and future of radiotherapy for the benefit of patients. Nat Rev Clin Oncol 10: 52–60.

Thomas AG, Liu W, Olkowski JL, Tang Z, Lin Q, Lu X-CM *et al.* (2001). Neuroprotection mediated by glutamate carboxypeptidase II (NAALADase) inhibition requires TGF-β. Eur J Pharmacol 430: 33–40.

Tolmachev V, Malmberg J, Estrada S, Eriksson O, Orlova A (2014). Development of a 124I-labeled version of the anti-PSMA monoclonal antibody capromab for immunoPET staging of prostate cancer: Aspects of labeling chemistry and biodistribution. Int J Oncol 44: 1998–2008.

Tong R, Coyle VJ, Tang L, Barger AM, Fan TM, Cheng J (2010). Polylactide nanoparticles containing stably incorporated cyanine dyes for in vitro and in vivo imaging applications. Microsc Res Tech 73: 901–909.

Tortella FC, Lin Y, Ved H, Slusher BS, Dave JR (2000). Neuroprotection produced by the NAALADase inhibitor 2-PMPA in rat cerebellar neurons. Eur J Pharmacol 402: 31–37.

Tse BW-C, Cowin GJ, Soekmadji C, Jovanovic L, Vasireddy RS, Ling M-T*et al.* (2015). PSMA-targeting iron oxide magnetic nanoparticles enhance MRI of preclinical prostate cancer. Nanomedicine 10: 375–386.

Tsukamoto T, Wozniak KM, Slusher BS (2007). Progress in the discovery and development of glutamate carboxypeptidase II inhibitors. Drug Discov Today 12: 767–776.

Vallabhajosula S, Goldsmith SJ, Kostakoglu L, Milowsky MI, Nanus DM, Bander NH (2005). Radioimmunotherapy of prostate cancer using 90Y-and 177Lu-labeled J591 monoclonal antibodies: effect of multiple treatments on myelotoxicity. Clin Cancer Res 11: 7195s–7200s.

Vallabhajosula S, Smith-Jones PM, Navarro V, Goldsmith SJ, Bander NH (2004). Radioimmunotherapy of prostate cancer in human xenografts using monoclonal antibodies specific to prostate specific membrane antigen (PSMA): studies in nude mice. Prostate 58: 145–155.

Van der Post J, De Visser S, De Kam M, Woelfler M, Hilt D, Vornov J *et al.* (2005). The central nervous system effects, pharmacokinetics and safety of the NAALADase-inhibitor GPI 5693. Br J Clin Pharmacol 60: 128–136.

Vittes GE, Harden EL, Ottensmeier CH, Rice J, Stevenson FK (2011). DNA fusion gene vaccines induce cytotoxic T-cell attack on naturally processed peptides of human prostate-specific membrane antigen. Eur J Immunol 41: 2447–2456.

Waeckerle-Men Y, Uetz-von Allmen E, Fopp M, von Moos R, Böhme C, Schmid H-P *et al.* (2006). Dendritic cell-based multi-epitope immunotherapy of hormone-refractory prostate carcinoma. Cancer Immunol Immunother 55: 1524–1533.

Wang H-l, Wang S-s, Song W-H, Pan Y, Yu H-p, Si T-G *et al.* (2015). Expression of prostate-specific membrane antigen in lung cancer cells and tumor neovasculature endothelial cells and its clinical significance. PLoS One 10: e0125924.

Wang H, Byun Y, Barinka C, Pullambhatla M, Hyo-eun CB, Fox JJ *et al.* (2010). Bioisosterism of urea-based GCPII inhibitors: synthesis and structure–activity relationship studies. Bioorg Med Chem Lett 20: 392–397.

Wang X, Huang SS, Heston WD, Guo H, Wang B-C, Basilion JP (2014). Development of targeted near-infrared imaging agents for prostate cancer. Mol Cancer Ther 13: 2595–2606.

Wang X, Ma D, Olson WC, Heston WD (2011). In vitro and in vivo responses of advanced prostate tumors to PSMA ADC, an auristatin-conjugated antibody to prostate-specific membrane antigen. Mol Cancer Ther 10: 1728–1739.

Watanabe R, Sato K, Hanaoka H, Harada T, Nakajima T, Kim I *et al.* (2014). Minibody-indocyanine green based activatable optical imaging probes: the role of short polyethylene glycol linkers. ACS Med Chem Lett 5: 411–415.

Watt F, Martorana A, Brookes DE, Ho T, Kingsley E, O'Keefe DS *et al.* (2001). A tissue-specific enhancer of the prostate-specific membrane antigen gene, FOLH1. Genomics 73: 243–254.

Weineisen M, Schottelius M, Simecek J, Baum RP, Yildiz A, Beykan S *et al.* (2015). 68Ga-and 177Lu-Labeled PSMA I&T: optimization of a PSMA-targeted theranostic concept and first proof-of-concept human studies. J Nucl Med 56: 1169–1176.

Weineisen M, Simecek J, Schottelius M, Schwaiger M, Wester H-J (2014). Synthesis and preclinical evaluation of DOTAGA-conjugated PSMA ligands for functional imaging and endoradiotherapy of prostate cancer. EJNMMI Res 1: 1–15.

Wernicke AG, Varma S, Greenwood EA, Christos PJ, Chao K, Liu H *et al.* (2014). Prostate-specific membrane antigen expression in tumor-associated vasculature of breast cancers. APMIS 122: 482–489.

Wiehr S, Bühler P, Gierschner D, Wolf P, Rolle AM, Kesenheimer C *et al.* (2014). Pharmacokinetics and PET imaging properties of two recombinant anti-PSMA antibody fragments in comparison to their parental antibody. Prostate 74: 743–755.

Williams BJ, Bhatia S, Adams LK, Boling S, Carroll JL, Li X-L *et al.* (2012). Dendritic cell based PSMA immunotherapy for prostate cancer using a CD40-targeted adenovirus vector. PLoS One 7: e46981.

Williamson LC, Neale JH (1988). Ultrastructural localization of N-acetylaspartylglutamate in synaptic vesicles of retinal neurons. Brain Res 456: 375–381.

Wissenbach U, Niemeyer BA, Fixemer T, Schneidewind A, Trost C, Cavalié A *et al.* (2001). Expression of CaT-like, a novel calcium-selective channel, correlates with the malignancy of prostate cancer. J Biol Chem 276: 19461–19468.

Witkin JM, Gasior M, Schad C, Zapata A, Shippenberg T, Hartman T *et al.* (2002). NAALADase (GCP II) inhibition prevents cocaine-kindled seizures. Neuropharmacology 43: 348–356.

Wright AS, Thomas LN, Douglas RC, Lazier CB, Rittmaster RS (1996). Relative potency of testosterone and dihydrotestosterone in preventing atrophy and apoptosis in the prostate of the castrated rat. J Clin Invest 98: 2558.

Wu LY, Johnson JM, Simmons JK, Mendes DE, Geruntho JJ, Liu T*et al.* (2014). Biochemical characterization of prostate-specific membrane antigen from canine prostate carcinoma cells. Prostate 74: 451–457.

Wu X, Ding B, Gao J, Wang H, Fan W, Wang X *et al.* (2011). Second-generation aptamer-conjugated PSMA-targeted delivery system for prostate cancer therapy. Int J Nanomedicine 6: 1747.

Wu Z-M, Zheng C-H, Zhu Z-H, Wu F-T, Ni G-L, Liang Y (2016). SiRNA-mediated serotonin transporter knockdown in the dorsal raphe nucleus rescues single prolonged stress-induced hippocampal autophagy in rats. J Neurol Sci 360: 133–140.

Xi H-B, Wang G-X, Fu B, Liu W-P, Li Y (2015). Survivin and PSMA loaded dendritic cell vaccine for the treatment of Prostate Cancer. Biol Pharm Bull 38: 827–835.

Xi Z-X, Kiyatkin M, Li X, Peng X-Q, Wiggins A, Spiller K *et al.* (2010a). N-acetylaspartylglutamate (NAAG) inhibits intravenous cocaine self-administration and cocaine-enhanced brain-stimulation reward in rats. Neuropharmacology 58: 304–313.

Xi ZX, Li X, Peng XQ, Li J, Chun L, Gardner EL *et al.* (2010b). Inhibition of NAALADase by 2-PMPA attenuates cocaine-induced relapse in rats: a NAAG-mGluR2/3-mediated mechanism. J Neurochem 112: 564–576.

Xiang B, Dong D-W, Shi N-Q, Gao W, Yang Z-Z, Cui Y*et al.* (2013). PSA-responsive and PSMA-mediated multifunctional liposomes for targeted therapy of prostate cancer. Biomaterials 34: 6976–6991.

Xu W, Siddiqui IA, Nihal M, Pilla S, Rosenthal K, Mukhtar H *et al.* (2013). Aptamer-conjugated and doxorubicin-loaded unimolecular micelles for targeted therapy of prostate cancer. Biomaterials 34: 5244–5253.

Yallapu MM, Khan S, Maher DM, Ebeling MC, Sundram V, Chauhan N *et al.* (2014). Anti-cancer activity of curcumin loaded nanoparticles in prostate cancer. Biomaterials 35: 8635–8648.

Yamamoto T, Hirasawa S, Wroblewska B, Grajkowska E, Zhou J, Kozikowski A *et al.* (2004). Antinociceptive effects of N-acetylaspartylglutamate (NAAG) peptidase inhibitors ZJ-11, ZJ-17 and ZJ-43 in the rat formalin test and in the rat neuropathic pain model. Eur J Neurosci 20: 483–494.

Yamamoto T, Kozikowski A, Zhou J, Neale JH (2008). Intracerebroventricular administration of N-acetylaspartylglutamate (NAAG) peptidase inhibitors is analgesic in inflammatory pain. Mol Pain 4: 1.

Yamamoto T, Nozaki-Taguchi N, Sakashita Y (2001a). Spinal N-acetyl-α-linked acidic dipeptidase (NAALADase) inhibition attenuates mechanical allodynia induced by paw carrageenan injection in the rat. Brain Res 909: 138–144.

Yamamoto T, Nozaki-Taguchi N, Sakashita Y, Inagaki T (2001b). Inhibition of spinal N-acetylated-α-linked acidic dipeptidase produces an antinociceptive effect in the rat formalin test. Neuroscience 102: 473–479.

Yamamoto T, Saito O, Aoe T, Bartolozzi A, Sarva J, Zhou J *et al.* (2007). Local administration of N-acetylaspartylglutamate (NAAG) peptidase inhibitors is analgesic in peripheral pain in rats. Eur J Neurosci 25: 147–158.

Yao V, Bacich DJ (2006). Prostate specific membrane antigen (PSMA) expression gives prostate cancer cells a growth advantage in a physiologically relevant folate environment in vitro. Prostate 66: 867–875.

Yao V, Berkman CE, Choi JK, O'Keefe DS, Bacich DJ (2010a). Expression of prostate-specific membrane antigen (PSMA), increases cell folate uptake and proliferation and suggests a novel role for PSMA in the uptake of the non-polyglutamated folate, folic acid. Prostate 70: 305–316.

Yao V, Berkman CE, Choi JK, O'Keefe DS, Bacich DJ (2010b). Expression of prostate-specific membrane antigen (PSMA), increases cell folate uptake and proliferation and suggests a novel role for PSMA in the uptake of the non-polyglutamated folate, folic acid. Prostate 70: 305–316.

Yao V, Parwani A, Maier C, Heston WD, Bacich DJ (2008). Moderate expression of prostate-specific membrane antigen, a tissue differentiation antigen and folate hydrolase, facilitates prostate carcinogenesis. Cancer Res 68: 9070–9077.

Youlin K, Li Z, Xin G, Mingchao X, Xiuheng L, Xiaodong W (2013). Enhanced function of cytotoxic T lymphocytes induced by dendritic cells modified with truncated PSMA and 4-1BBL. Hum Vaccines Immunother 9: 766–772.

Yu YJ, Atwal JK, Zhang Y, Tong RK, Wildsmith KR, Tan C *et al.* (2014). Therapeutic bispecific antibodies cross the blood–brain barrier in nonhuman primates. Sci Transl Med 6: 261ra154–261ra154.

Zechmann CM, Afshar-Oromieh A, Armor T, Stubbs JB, Mier W, Hadaschik B *et al.* (2014). Radiation dosimetry and first therapy results with a 124I/131I-labeled small molecule (MIP-1095) targeting PSMA for prostate cancer therapy. Eur J Nucl Med Mol Imaging 41: 1280–1292.

Zhang Y, Guo Z, Du T, Chen J, Wang W, Xu K *et al.* (2013). Prostate specific membrane antigen (PSMA): a novel modulator of p38 for proliferation, migration, and survival in prostate cancer cells. Prostate 73: 835–841.

Zhao J, Ramadan E, Cappiello M, Wroblewska B, Bzdega T, Neale JH (2001). NAAG inhibits KCl-induced [3H]-GABA release via mGluR3, cAMP, PKA and L-type calcium conductance. Eur J Neurosci 13: 340–346.

Zhao R, Matherly LH, Goldman ID (2009). Membrane transporters and folate homeostasis: intestinal absorption and transport into systemic compartments and tissues. Expert Rev Mol Med 11: e4.

Zhao Y, Duan S, Zeng X, Liu C, Davies NM, Li B *et al.* (2012). Prodrug strategy for PSMA-targeted delivery of TGX-221 to prostate cancer cells. Mol Pharm 9: 1705–1716.

Zhong C, Luo Q, Jiang J (2014). Blockade of N-acetylaspartylglutamate peptidases: a novel protective strategy for brain injuries and neurological disorders. Int J Neurosci 124: 867–873.

Zhong C, Zhao X, Sarva J, Kozikowski A, Neale JH, Lyeth BG (2005). NAAG peptidase inhibitor reduces acute neuronal degeneration and astrocyte damage following lateral fluid percussion TBI in rats. J Neurotrauma 22: 266–276.

Zhong C, Zhao X, Van KC, Bzdega T, Smyth A, Zhou J *et al.* (2006). NAAG peptidase inhibitor increases dialysate NAAG and reduces glutamate, aspartate and GABA levels in the dorsal hippocampus following fluid percussion injury in the rat. J Neurochem 97: 1015–1025.

Zhou Z, Lane MV, Kemppainen JA, French FS, Wilson EM (1995). Specificity of ligand-dependent androgen receptor stabilization: Receptor domain interactions influence ligand dissociation and receptor stability. Mol Endocrinol 9: 208–218.

Zhu Y, Sun Y, Chen Y, Liu W, Jiang J, Guan W*et al.* (2015). In vivo molecular MRI imaging of prostate cancer by targeting PSMA with polypeptide-labeled superparamagnetic iron oxide nanoparticles. Int J Mol Sci 16: 9573–9587.

Zuccolotto G, Fracasso G, Merlo A, Montagner IM, Rondina M, Bobisse S *et al.* (2014). PSMA-specific CAR-engineered T cells eradicate disseminated prostate cancer in preclinical models.

Zuo D, Wang C, Li Z, Lin L, Duan Z, Qi H *et al.* (2014). Existence of glia mitigated ketamine-induced neurotoxicity in neuron–glia mixed cultures of neonatal rat cortex and the glia-mediated protective effect of 2-PMPA. Neurotoxicology 44: 218–230.